




Pioneering first-in-class FAAH-HDAC inhibitors as potential multitarget neuroprotective agents

Alessandro Papa¹ | Ilaria Cursaro¹  | Luca Pozzetti¹ | Chiara Contri² |
Martina Cappello² | Silvia Pasquini³  | Gabriele Carullo¹ | Anna Ramunno⁴ |
Sandra Gemma¹ | Katia Varani² | Stefania Butini¹  | Giuseppe Campiani¹ |
Fabrizio Vincenzi²

¹Department of Biotechnology, Chemistry and Pharmacy, University of Siena, Siena, Italy

²Department of Translational Medicine, University of Ferrara, Ferrara, Italy

³Department of Chemical, Pharmaceutical and Agricultural Sciences, University of Ferrara, Ferrara, Italy

⁴Department of Pharmacy, University of Salerno, Fisciano, Italy

Correspondence

Stefania Butini, Department of Biotechnology, Chemistry and Pharmacy, University of Siena, Siena 53100, Italy.

Email: butini3@unisi.it

Funding information

MIUR-PRIN, Grant/Award Number: n° 20175SA5JJ; Ministry of University and Research (MUR) National Recovery and Resilience Plan (NRRP), Grant/Award Number: PE00000006 CUP H93C22000660006

Abstract

Aiming to simultaneously modulate the endocannabinoid system (ECS) functions and the epigenetic machinery, we selected the fatty acid amide hydrolase (FAAH) and histone deacetylase (HDAC) enzymes as desired targets to develop potential neuroprotective multitarget-directed ligands (MTDLs), expecting to achieve an additive or synergistic therapeutic effect in oxidative stress-related conditions. We herein report the design, synthesis, and biological evaluation of the first-in-class FAAH-HDAC multitarget inhibitors. A pharmacophore merging strategy was applied, yielding 1-phenylpyrrole-based compounds **4a–j**. The best-performing compounds (**4c**, **4f**, and **4h**) were tested for their neuroprotective properties in oxidative stress models, employing 1321N1 *human* astrocytoma cells and SHSY5 *human* neuronal cells. In our preliminary studies, compound **4h** stood out, showing a balanced nanomolar inhibitory activity against the selected targets and outperforming the standard antioxidant *N*-acetylcysteine *in vitro*. Together with **4f**, **4h** was also able to protect 1321N1 cells from *tert*-butyl hydroperoxide or glutamate insult. Our study may provide the basis for the development of novel MTDLs targeting the ECS and epigenetic enzymes.

KEYWORDS

fatty acid amide hydrolase, histone deacetylase, multitarget-directed ligands, neuroprotection, oxidative stress

1 | INTRODUCTION

In recent years, the design of multitarget drugs has gained momentum, defying the classic medicinal chemistry paradigm of “one drug, one target” that has often revealed its drawbacks, especially for the

treatment of complex and multifactorial diseases. Hence, polypharmacology has emerged as a promising approach in drug discovery that exploits a multitarget drug hitting different biological targets through multiple modes of action, while avoiding off-target liabilities associated with the multidrug combination therapy.^[1–3] Polypharmacology offers

Alessandro Papa and Ilaria Cursaro co-first authors.

Giuseppe Campiani and Fabrizio Vincenzi are co-last authors.

This is an open access article under the terms of the Creative Commons Attribution-NonCommercial-NoDerivs License, which permits use and distribution in any medium, provided the original work is properly cited, the use is non-commercial and no modifications or adaptations are made.

© 2023 The Authors. *Archiv der Pharmazie* published by Wiley-VCH GmbH on behalf of Deutsche Pharmazeutische Gesellschaft.

various benefits, including improving treatment efficacy through additional or synergistic pharmacodynamic effects, reducing the onset of drug resistance, and minimizing adverse effects.^[1] Further, multitarget-directed ligands (MTDLs)^[4,5] offer beneficial pharmacokinetic advantages and avoid the drug–drug interaction issues of drug combinations. MTDLs can be described as molecular hybrids endowed with the key pharmacophoric features required to modulate two or more biological targets while preserving and combining the original therapeutic values. The fundamental moieties can be linked, fused, or merged depending on the presence and the type of tethering linkage.^[4] This approach can be favorably applied for the treatment of multifactorial pathological conditions, such as cancer and neurological disorders. In this context, aiming to tackle central nervous system (CNS) disorders, we decided to pursue this innovative polypharmacological strategy by combining the well-known antineuroinflammatory activity mediated by the endocannabinoid system (ECS) with the emerging neuroprotective effect of small-molecule epigenetic modulators targeting histone deacetylases (HDACs).^[2,6] The ECS is an extensive homeostatic neuromodulatory system mainly involved in the development and plasticity of the CNS, the antinociceptive response to noxious stimuli, and the regulation of metabolic energy balance and immune response.^[7,8] It is also remarkably involved in inflammation and neurodegeneration.^[9–11] The ECS is comprised of G protein-coupled cannabinoid receptors type 1 and type 2 (CB₁R and CB₂R), their endogenous arachidonate-based ligands, known as endocannabinoids (eCBs), and the two main catabolic enzymes, namely fatty acid amide hydrolase (FAAH) and monoacylglycerol lipase (MAGL).

FAAH is a serine hydrolase enzyme that metabolizes several eCBs, including anandamide (AEA). Its pharmacological inhibition determines an indirect stimulation of the CBRs, promoting eCBs retrograde signalling.^[2] This neuromodulation results in a neuroprotective effect attained through different mechanisms, such as prevention of excitotoxicity, reduction of Ca²⁺ pre- and postsynaptic influx, antioxidant activity, and suppression of cytokine production.^[11–13]

Recently, we disclosed wide libraries of carbamate-based FAAH inhibitors (FAAHis).^[14–17] These derivatives share a common pharmacophore that combines an electrophilic center undergoing nucleophilic attack by the catalytic Ser241, a suitably decorated biaryl leaving group, and a lateral chain that can exhibit various levels of lipophilicity to mimic the AEA apolar tail. Among them, the 1-phenylpyrrolic compound **1** (mFAAH IC₅₀ = 0.60 nM, hFAAH IC₅₀ = 3.72 nM, Figure 1) emerged as a potent and selective FAAHi endowed with *in vivo* efficacy in a murine model of epilepsy.^[14] To improve the physicochemical properties of this type of derivative, we subsequently developed a novel series of derivatives characterized by more polar and protonatable lateral chains, as exemplified by compound **2** (hFAAH IC₅₀ = 10.1 ± 0.6 nM, Figure 1), which showed a marked anti-inflammatory and neuroprotective profile in hippocampal rat explants.^[17]

Epigenetic regulation plays a pivotal role in virtually every biological process. The alteration of HDAC levels is associated with the onset and development of various diseases, including cancer, genetic disorders such as Rett syndrome, Charcot–Marie–Tooth disease and retinitis pigmentosa, as well as idiopathic pulmonary

fibrosis, and several neurodegenerative diseases.^[18] HDAC inhibitors (HDACis) not only proved to be beneficial in several cellular and animal models of the aforementioned diseases, but they also emerged as promising neuroprotective agents in neuronal models of oxidative stress induced by glutathione depletion.^[6,19–26] The HDAC superfamily consists of 18 isoforms, classified into four classes based on sequence homology. Among them, three are zinc-dependent enzymes (Class I, IIA, and IIB, IV), while Class III HDACs are nicotinamide adenine dinucleotide (NAD⁺)-dependent enzymes and are referred to as sirtuins.^[27] So far, medicinal chemistry efforts have primarily focused on the development of selective HDAC6is and Class I HDACis, as these isoforms remain the most thoroughly investigated. The pharmacophore of zinc-dependent HDACis consists of three main structural elements: a cap group that interacts with surface residues, a zinc-binding group (ZBG) that chelates the metal cation in the active site, and a linker, tethering the cap group and ZBG. Hydroxamic acids are often used as the ZBG since they have a strong zinc chelation ability.^[28,29] Encompassing various binding modes in the HDAC isoforms the linker moiety occupies a hydrophobic channel that connects the catalytic site to the outer surface. Isoform selectivity and potency of HDACis heavily depend on the structure of the selected ZBG and cap group. In addition to the abovementioned carbamate-based FAAHis, the privileged 1-phenylpyrrole scaffold was explored as a cap group for the development of hydroxamate-based HDACis, as demonstrated by our work with compound **3** (Figure 1).^[30]

In the frame of our research interest in the development of MTDLs for treating CNS diseases,^[31–36] we recently exploited the ECS modulation for developing different classes of MTDLs, such as MAGL/FAAH dual inhibitors^[37] and FAAH/D3 modulators.^[16] Our expertise in the design of HDACis^[21,38,39] and their emerging protecting role against oxidative stress^[40] inspired the development of novel modulators of both the ECS and epigenetic regulation as potential neuroprotective agents.

We herein describe the design, synthesis, and biological evaluation of the first-in-class FAAH–HDAC MTDLs. The previously mentioned FAAHis and HDACi (**1–3**) exhibited partial structural motifs required for the inhibition of both targets and hinged on the same 1-phenylpyrrole skeleton, which could be easily accommodated within the enzymes' active sites. Hence, starting from this biaryl privileged scaffold, we rationally designed and synthesized two series of hybrid compounds, namely **4a–f** and **4g–j** (Figure 1 and Table 1). We pursued a pharmacophore merging design strategy to fulfill both pharmacophoric requirements. To achieve this, a hydroxamic acid ZBG—essential for HDAC inhibition—was embedded into the structure of the FAAHis **1** and **2**, which in line with literature perspectives, could serve as cap/linker groups.^[18]

Of note, **1** and **2** already comprise the electrophilic function needed for the covalent inhibition of the FAAH enzyme. In the first set of compounds (**4a–f**), the ZBG moiety replaced the carboxamide group on the pyrrole ring, while for the second set (**4g–j**) we designed “inverted” analogs bearing the hydroxamic acid on the terminal phenyl ring of the lateral chain. Hence, the influence of the ZBG position on the potency and selectivity against the selected biological targets was

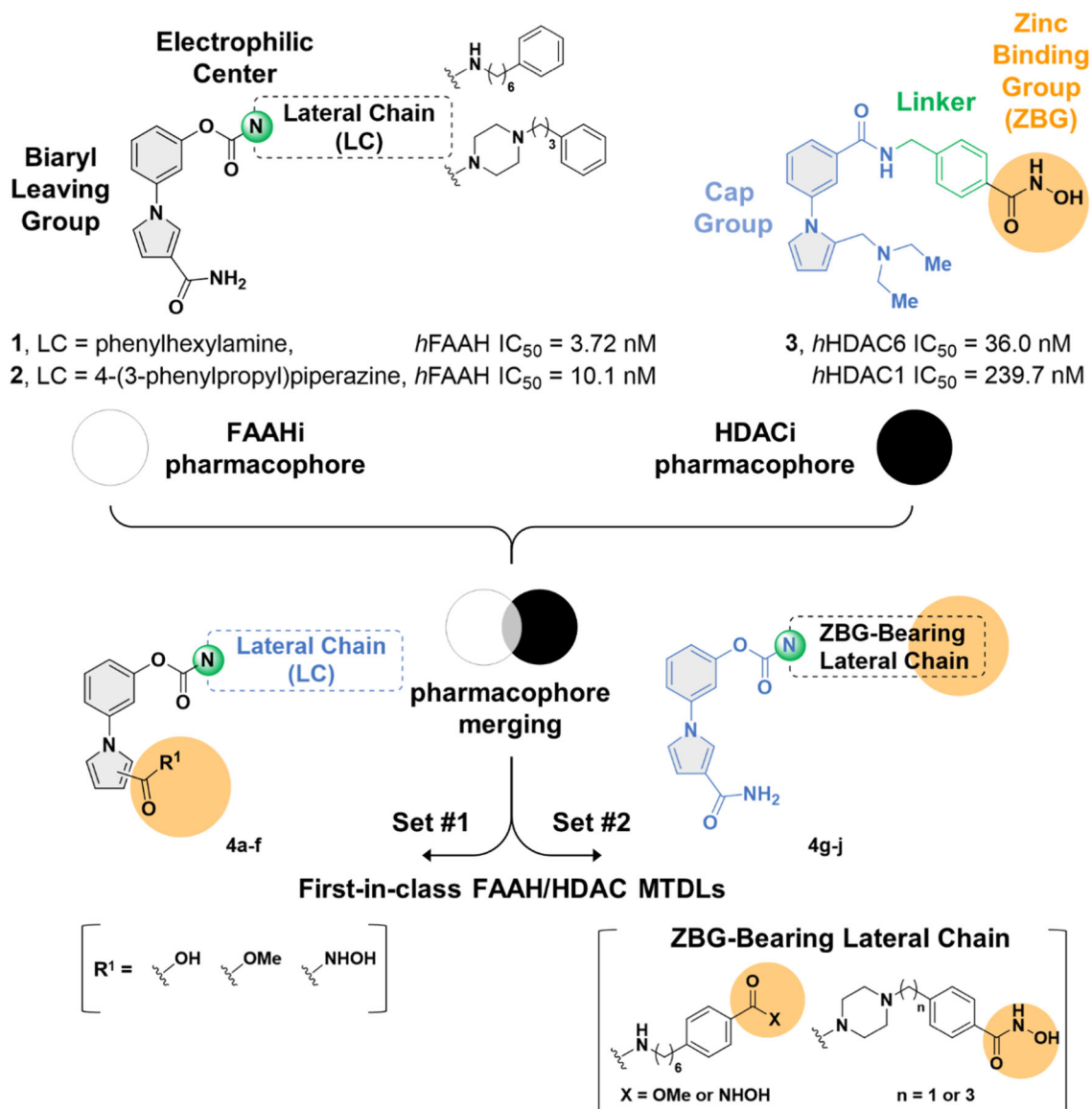


FIGURE 1 Rational design of FAAH/HDAC MTDLs by applying a pharmacophore merging strategy, starting from the structural analysis of phenylpyrrole-based FAAH inhibitors **1** and **2** and HDAC inhibitor **3**. FAAHi, FAAH inhibitor; HDACi, HDAC inhibitor.

evaluated by enzymatic assays. Moreover, synthetic efforts yielded both hydroxamic acids **4c,d,f,h-j**, and carboxylic acids **4b,e**. Although carboxylic acids are poorly represented as HDAC-specific ZBG—usually leading to weak enzymatic inhibition—some of the HDACis initially discovered (e.g., butyric acid, valproic acid, and phenylbutyric acid) bear this moiety.^[41] This may constitute a worthwhile modification to improve the water solubility and reduce the toxicity associated with the hydroxamic moiety.^[42] We also prepared the methyl ester analogs (**4a,g**) of the hydroxamic acid-bearing inhibitors **4c,h** as negative controls for HDAC inhibition. Initially, the newly synthesized compounds were tested against FAAH and HDAC6, selecting this peculiar HDAC isoform due to its major involvement in oxidative stress-related CNS diseases.^[40] The selectivity profile of the most promising compounds was assessed by testing them against *hHDAC*

isoforms **1**, **8**, **10**, and *hMAGL*, as reported in Table 2. The experimental results were rationalized by computational studies, performed by applying a docking protocol against FAAH and HDAC6 enzymes. Additionally, selected compounds were tested for their neuroprotective properties against oxidative stress induced in 1321N1 astrocyte and SH-SY5Y neuronal cell lines.

2 | RESULTS AND DISCUSSION

2.1 | Chemistry

The title carbamate-based FAAH-HDACis **4a-j** can be synthesized by using a convergent approach, combining aminic synthons with

TABLE 1 Inhibitory activity of the novel compounds 4a–j on human (h) FAAH and human (h) HDAC6 enzymes.

Cpd	Structure	hFAAH IC ₅₀ (nM) ^a	hHDAC6 IC ₅₀ (nM) ^a
4a		6.75 ± 0.47	>10,000 (1%)
4b		28.3 ± 1.8	>10,000 (8%)
4c		15.9 ± 1.2	3999 ± 312
4d		65.6 ± 4.7	>10,000 (6%)
4e		1817 ± 154	>10,000 (3%)
4f		36.2 ± 3.2	1387 ± 108
4g		30.7 ± 2.2	>10,000 (1%)
4h		297 ± 17	370 ± 23
4i		>10,000 (21%)	78.4 ± 5.1
4j		>10,000 (17%)	112 ± 7
1	-	3.72 ± 0.21 ^[15]	-
2	-	10.1 ± 0.6 ^[17]	-
3	-	-	36.0 ± 2.9 ^[30]

Abbreviations: FAAH, fatty acid amide hydrolase; HDAC, histone deacetylase.

^aData are expressed as mean ± SEM of three independent experiments performed in triplicate. Data in parentheses indicates inhibition at the 10 μM concentration. Incubation time = 30 min.

suitable phenolic derivatives. If required, a final step of debenzoylation or tetrahydropyranyl (THP) deprotection is envisaged to obtain the desired target compounds.

In Scheme 1 the synthesis of amines **14a,b** is depicted. Methyl 4-(bromomethyl)benzoate **5** was refluxed in toluene in the presence of triphenylphosphine to obtain the Wittig salt **6**. The commercially available 5-aminopentan-1-ol **7** was converted into the phthalimido derivative **8**, which was subsequently oxidized to the corresponding aldehyde **9** via a

2,2,6,6-tetramethylpiperidine 1-oxyl (TEMPO)-catalyzed reaction. This latter reacted with the Wittig salt **6** in the presence of potassium bis(trimethylsilyl)amide (KHMDS) to afford olefine **10**. A palladium-catalyzed hydrogenation furnished intermediate **11**, which was then hydrolyzed to the carboxylic acid **12**. Treatment of **12** with thionyl chloride and subsequent reaction with *O*-benzylhydroxylamine hydrochloride generated the key protected hydroxamic acid **13**. Final phthalimide removal, by means of hydrazine monohydrate, on compounds **11** and **13** furnished amines **14a** and **14b**, respectively.

The synthesis of amines **14c,d** is depicted in Scheme 2. Ethyl-4-iodobenzoate **15** was subjected to a Heck-type alkylation in the presence of allyl alcohol and palladium acetate furnishing compound **16**, which was reacted, under reductive amination conditions, with 1-Cbz-piperazine to give intermediate **17**. The ethyl ester **17** was then hydrolyzed to carboxylic acid **18**, which was converted into the corresponding *O*-THP-protected hydroxamic acid **19**. The final cleavage of the Cbz group furnished the free amine **14c**. For the synthesis of **14d** 4-(bromomethyl)benzoic acid **20** was converted into the corresponding *O*-THP-protected intermediate **21**. This latter was finally alkylated in the presence of piperazine to obtain **14d**.

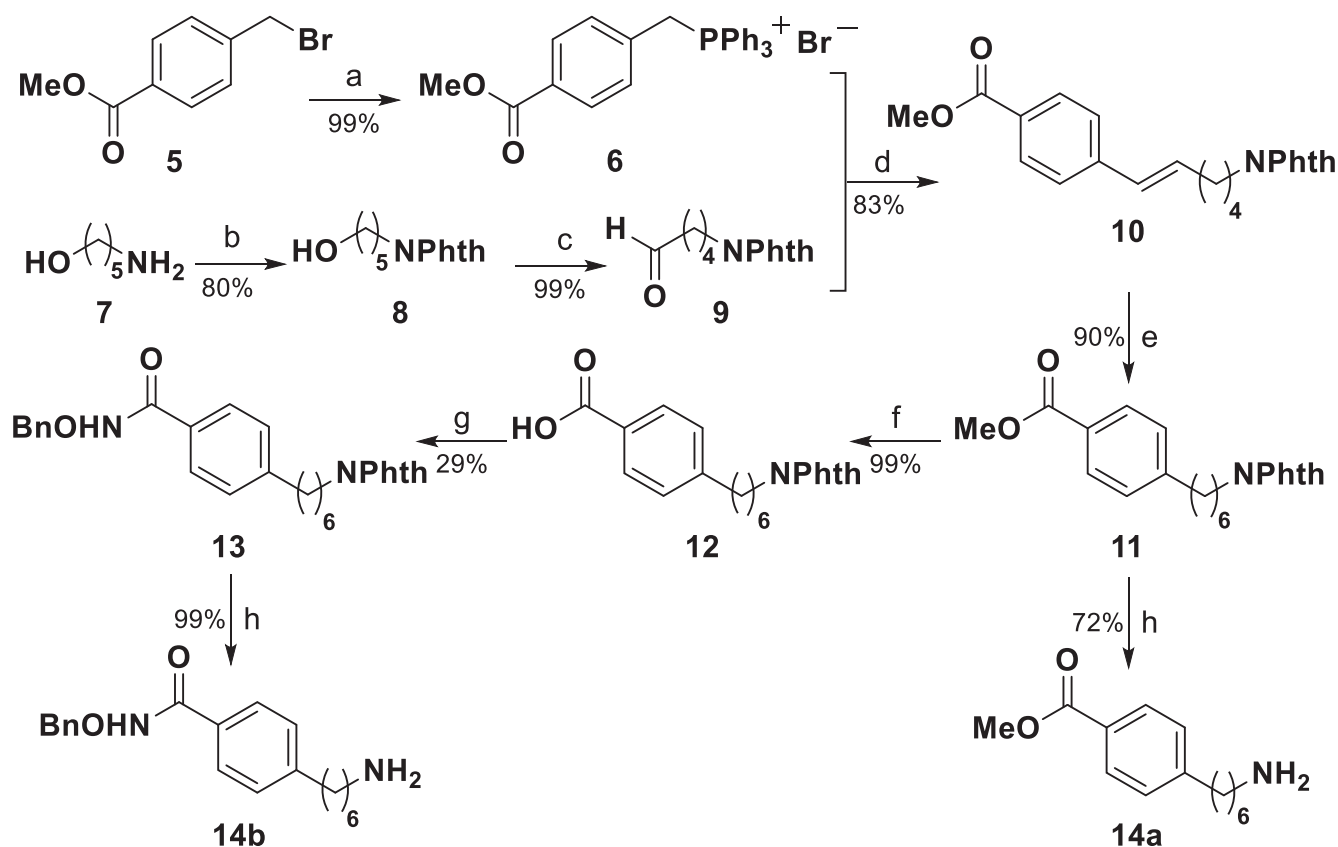
In Scheme 3, the synthesis of phenols **23a-d** is displayed. Treatment of the previously reported 1-(3-hydroxyphenyl)-1*H*-pyrrole-3-carboxylic acid **22**^[14] with trimethylsilyl chloride (TMSCl)

TABLE 2 Selectivity profile of compounds **4c,f,h** on isoforms 1, 8, 10 of human HDAC and on human MAGL enzymes.

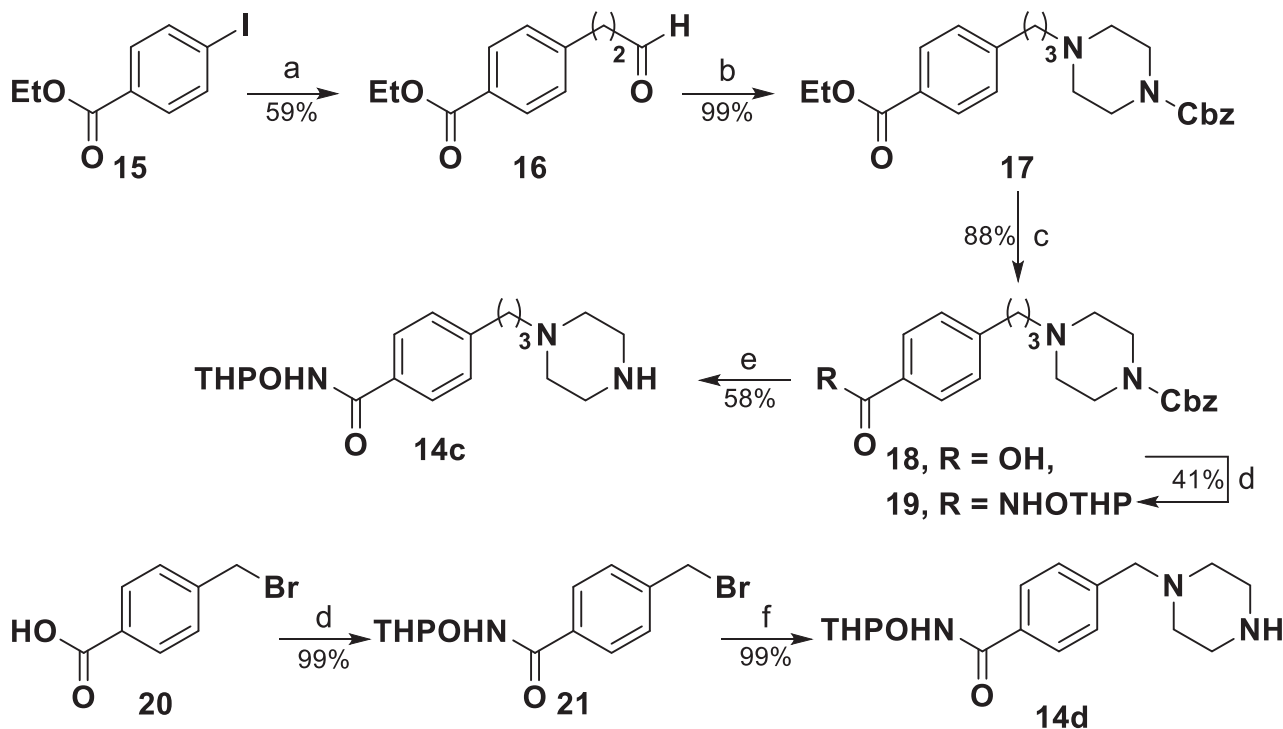
Cpd	hMAGL IC ₅₀ (nM) ^a	hHDAC1 IC ₅₀ (nM) ^a	hHDAC8 IC ₅₀ (nM) ^a	hHDAC10 IC ₅₀ (nM) ^a
4c	>10,000	>10,000	6350 ± 412	>10,000
4f	>10,000	>10,000	>10,000	9050 ± 651
4h	>10,000	531 ± 26	1410 ± 116	659 ± 37
3 ^[30]	-	239.7 ± 38.2	n.t.	n.t.

Abbreviations: HDAC, histone deacetylase; MAGL, monoacylglycerol lipase; n.t., not tested.

^aData are expressed as mean ± SEM of three independent experiments performed in triplicate. Incubation time = 30 min.



SCHEME 1 Synthesis of amines **14a,b**. Reagents and conditions: (a) PPh₃, dry toluene, 110°C, 16 h, 99%; (b) phthalic anhydride, dry toluene, 110°C, 24 h, 80%; (c) TEMPO, trichloroisocyanuric acid (TCICA), dry DCM, 0°C, 15 min, 99%; (d) KHMDS, dry THF, 0–25°C, 16 h, 83%; (e) H₂, Pd/C, EtOAc/MeOH, 25°C, 1 h, 90%; (f) 0.1 N NaOH solution, THF, 25°C, 16 h, 99%; (g) SOCl₂, dry THF, 70°C, 2 h, *O*-benzylhydroxylamine hydrochloride, DIPEA, dry DCM, 25°C, 16 h, 29%; (h) hydrazine monohydrate, EtOH, 78°C, 1 h, 72%–99%.



SCHEME 2 Synthesis of amines **14c,d**. Reagents and conditions: (a) allyl alcohol, Pd(OAc)₂, NaHCO₃, tetrabutylammonium bromide (TBAB), dry DMF, 80°C, 3 h, 59%; (b) 1-Cbz-piperazine, NaBH₃CN, dry MeOH, 0–25°C, 16 h, 99%; (c) 0.1 N NaOH solution, THF, 16 h, 88%; (d) *O*-(tetrahydro-2*H*-pyran-2-yl)hydroxylamine, EDC-HCl, dry DCM/dry DMF, 25°C, 18 h, 41% for **19** and 99% for **21**; (e) H₂, Pd/C, MeOH, 25°C, 3 h, 58%; (f) piperazine, K₂CO₃, dry THF, 65°C, 16 h, 99%.

in methanol or benzyl bromide in DMF furnished the ester derivatives **23a** and **23b**, respectively.

Vilsmeier–Haack formylation of (1*H*-pyrrol-1-yl)phenol **24**^[43] furnished the 2-carboxyaldehyde derivative **25a**. This latter and the previously reported 3-carboxyaldehyde isomer **25b**^[14] were reacted with methoxymethyl (MOM) chloride to form the corresponding MOM-protected intermediates **26a,b**. Subsequently, the Pinnick oxidation protocol was applied to compounds **26a,b** and yielded the corresponding carboxylic acids **27a,b**, which were treated with *O*-benzylhydroxylamine hydrochloride and bis(2-oxo-3-oxazolidinyl)phosphinic chloride (BOP-Cl) to give the protected hydroxamic acids **28a,b**. The synthons **23c,d** were obtained by selective deprotection of MOM ether on compounds **28a,b**.

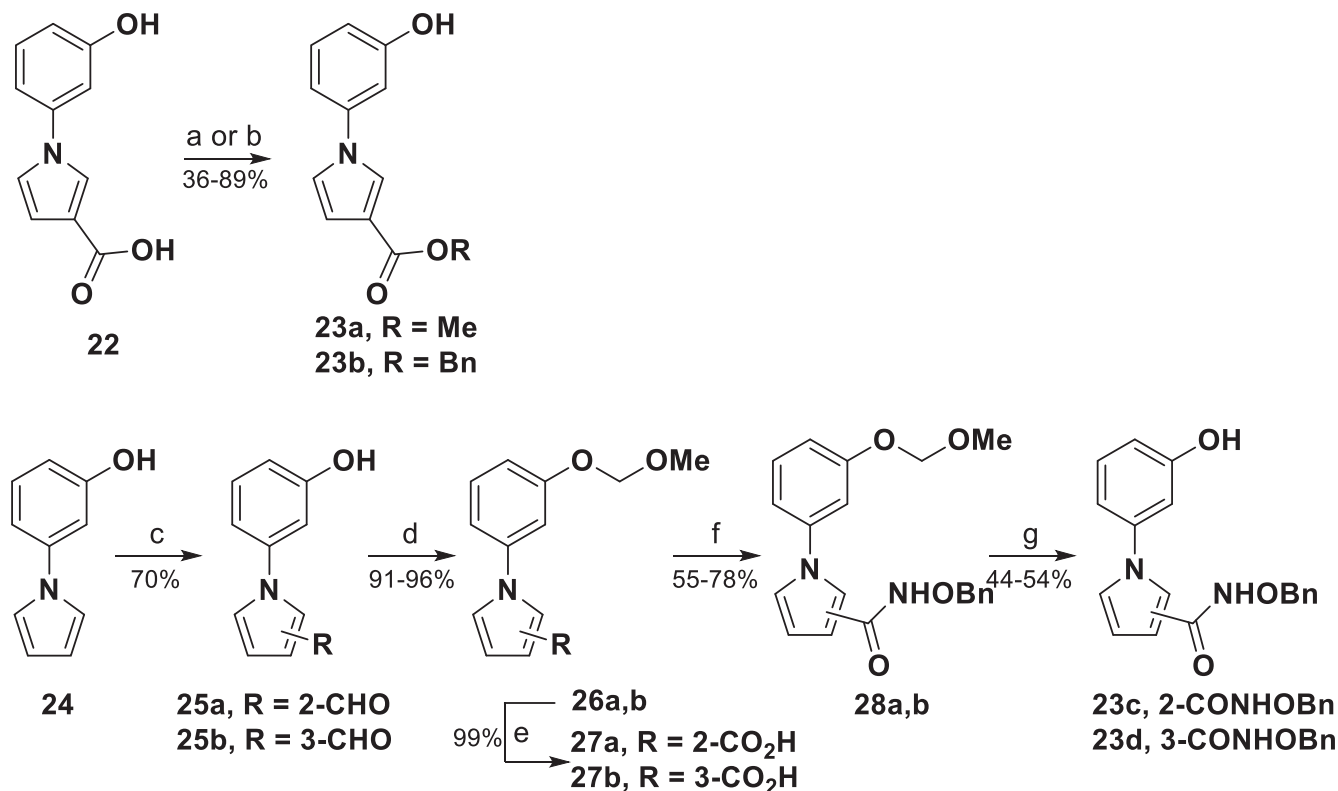
The final steps for the synthesis of **4a–f** and **4g–j**, respectively, bearing the ZBG moiety on the pyrrole ring (first set) or in the *para*-position of the lateral chain terminal phenyl ring (second set) are described in Schemes 4 and 5. The previously reported 6-phenylhexylamine (**14e**) or 1-(3-phenylpropyl)piperazine (**14f**), together with newly developed amines **14a–d** were combined with phenols **23a–d** (Schemes 4) and 1-(3-hydroxyphenyl)-1*H*-pyrrole-3-carboxamide **23e** (Scheme 5) in presence of 4-nitrophenyl chloroformate to obtain the respective carbamate-based derivatives. Briefly, in Scheme 4, amine **14e** was combined with phenols **23a–d** to obtain target compound **4a** and intermediates **29a–c**. By reacting amine **14f** with phenols **23b** and **23d**, compounds **30a,b** were obtained. Intermediates **29a–c** and **30a,b** underwent final palladium-catalyzed hydrogenation, furnishing target

compounds **4b–f**. In Scheme 5, by combining amine **14a** with phenol **23e**, compound **4g** was obtained. Amines **14b–d** reacted with phenol **23e** to form intermediates **31a–c**. *O*-Benzyl-protected intermediate **31a** was subjected to a palladium-catalyzed hydrogenation furnishing target compound **4h**, while THP removal from intermediates **31b,c** under acidic conditions yielded compounds **4i,j**.

2.2 | Biological evaluation and computational studies

2.2.1 | Enzymatic assays and structure-activity relationship discussion

The multitarget inhibitory profile of the newly synthesized compounds was primarily assessed by evaluating their half-maximal inhibitory concentration (IC₅₀) values against *human* FAAH and HDAC6 *in vitro*. FAAH inhibition activity was measured on a *human* recombinant purified enzyme following a 30 min preincubation with the tested compounds. The IC₅₀ values versus the target enzymes are reported in Table 1 for derivatives **4a–j**, taking compounds **1–3** as the reference compounds. The purpose of our screening was to identify a compound with a well-balanced inhibitory profile since an ideal MTDL should equally inhibit the selected targets. Indeed, an imbalance in the inhibitory potency ratio would lead to differing levels of receptor occupancy *in vivo*, requiring an increased dosage to attain the beneficial multitarget effects.^[44,45]



SCHEME 3 Synthesis of phenols **23a-d**. Reagent and conditions: (a) TMSCl, MeOH, 0°C to 25°C, 14 h, 89% (for **23a**); (b) benzyl bromide, NaHCO₃, dry DMF, 40°C, 16 h, 36% (for **23b**); (c) oxalyl chloride, DMF solution in dry DCM, dry DCM, 0–40°C, 3 h, then 1 N NaOH, 25°C, 16 h, 70%; (d) MOM-Cl, DIPEA, dry DCM, 0°C, 1 h, 91%–96%; (e) NaClO₂ saturated solution, NaH₂PO₄ saturated solution, 2-methyl-2-butene, *t*-BuOH, 25°C, 16 h, 99%; (f) *O*-benzylhydroxylamine hydrochloride, BOP-Cl, TEA, dry THF, 25°C, 16 h, 55%–78%; (g) 1 N HCl/MeOH, MeOH, 25°C, 16 h, 44%–54%.

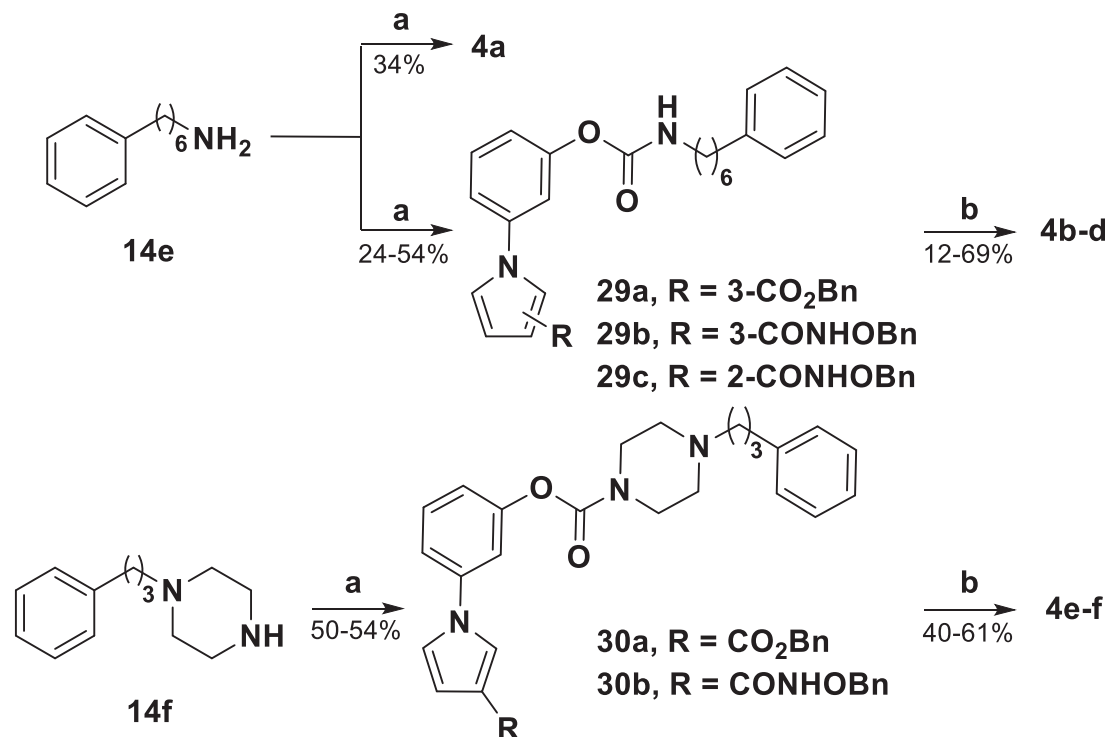
The selective FAAH inhibitory activity of compounds **4a,b,e,g** could be attributed to the lack of a ZBG or to the presence of a weak ZBG (i.e., carboxylic acid). Compound **4d** exhibited the same inhibitory profile, probably owing to its distinct geometry. Unexpectedly, compounds **4i,j** completely lost their activity against FAAH and were only able to inhibit HDAC6. Compounds **4c,f,h** emerged as the most promising MTDLs as their IC₅₀ on both targets lay in the nanomolar or low-micromolar range. In particular, **4h** showed comparable potencies against the two enzymes. Thus, we selected compounds **4c,f,h** as the hit compounds. Further investigations were carried out to assess their selectivity profile (Table 2), their potential antioxidant and neuroprotective effects (Figure 6 and Supporting Information: Table S1), their solubility and chemical stability profiles, along with selected predicted ADME properties (Supporting Information: Tables S2–S4). Although the *in silico* pharmacokinetic data were not fully satisfactory, the biological evaluation highlighted the promising pharmacological application of these first-in-class MTDLs as neuroprotective agents.

2.2.2 | Molecular docking studies

Computational studies were performed using the crystal structures of FAAH (PDB code: 3K84, chain A)^[46] and HDAC6 (PDB code:

5EDU, chain A),^[47] by applying the docking protocol described in Section 4. All molecules were docked on HDAC6 owing to their higher inhibitory potency against this isoform and the most remarkable docking results are herein discussed. Regarding FAAH, all the newly developed inhibitors exploit the pharmacophore of our previously reported reference compounds **1** and **2**, whose interactions in the binding pocket are typified by the docking pose of compound **1**, as depicted in Figure 2a. Briefly, the electrophilic carbon of the carbamate is placed in proximity of the catalytic Ser241 hydroxyl oxygen, while the carbonyl oxygen engages in a series of stabilizing H-bonds within the nitrogen-rich oxyanion hole composed of Ile238, Gly239, and Gly240. At the same time, the phenyl-pyrrole core occupies the solvent-exposed cytoplasmic access (CA) channel, thus allowing the 3-CONH₂ substituent to establish an H-bond with the L380 backbone. Finally, the lateral chain is accommodated in the acyl chain-binding (ACB) pocket, where it interacts with the hydrophobic residues Phe192, Tyr194, Leu380, Phe381, Phe432, and Val491.

The great inhibitory potency against FAAH of the first set of compounds (**4a-f**) is confirmed by their docking poses, which mimic the binding mode described for the reference compound **1**. Compound **4a**, bearing a methyl ester moiety, resulted in the most potent FAAHi of the whole series (IC₅₀ = 6.75 ± 0.47 nM, Table 1),



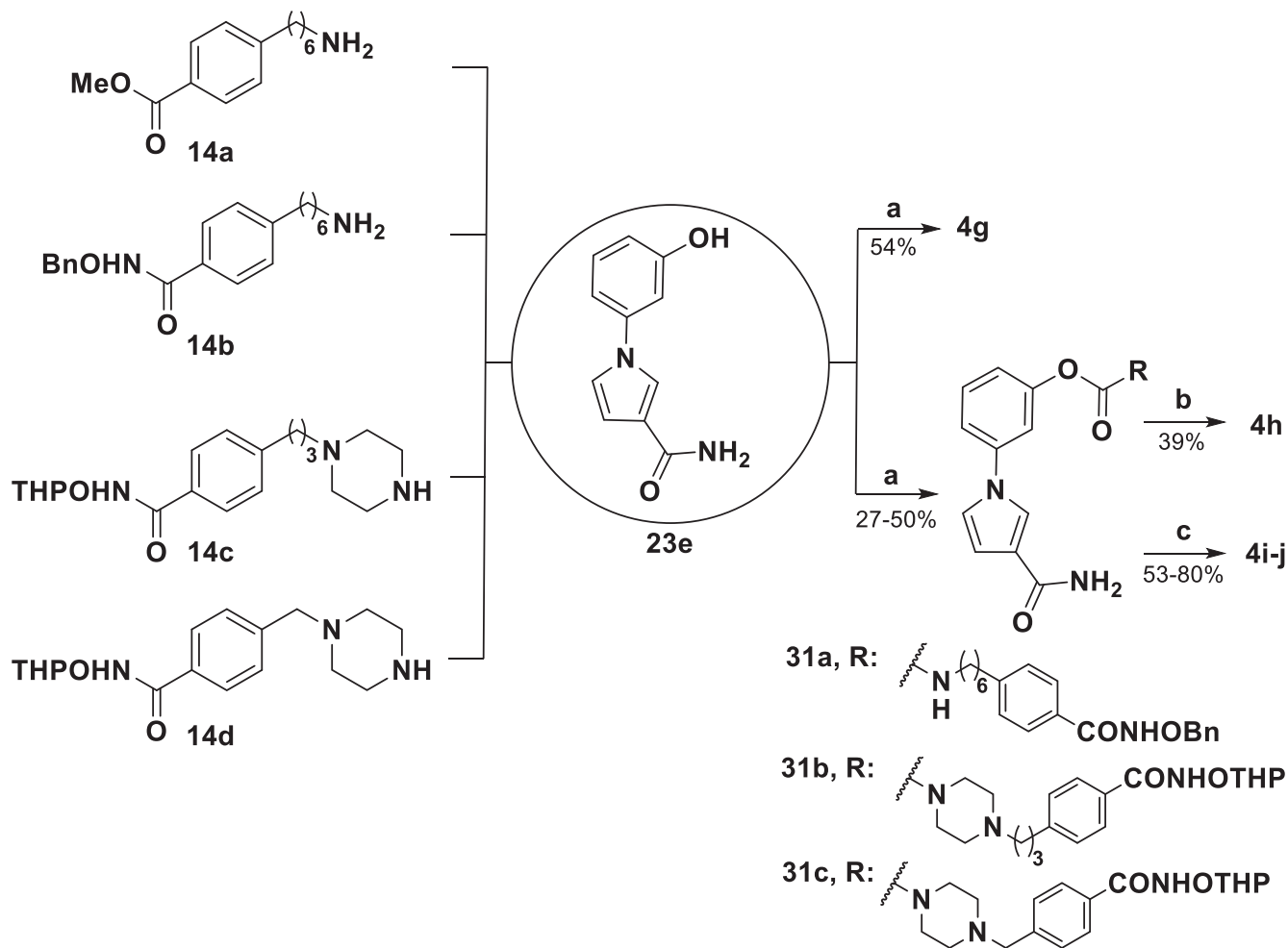
SCHEME 4 Synthesis of the first set of title compounds (**4a–f**). Reagents and conditions: (a) 4-nitrophenyl chloroformate, dry TEA, dry DCM, and suitable phenol **23a–d**, 0°C, 3 h, then amine **14e,f**, 25°C, 3 h, 24%–54%; (b) H₂, Pd/C, MeOH/EtOAc, 25°C, 2 h, 12%–69%.

while the corresponding more polar carboxylic acid **4b** and the hydroxamic acids **4c,d** still retained an excellent low nanomolar activity. These small variations in terms of activity could be ascribed to a different orientation of the substituted pyrrole system. As shown in Figure 2b–d, the more polar substituents of compounds **4b,c** point toward the solvent-exposed entrance of the CA channel, thus establishing an H-bond with Gln273. On the other hand, the bulkier and more lipophilic methyl ester **4a** is buried within the channel determining a flip of the pyrrole ring. The tertiarization of the carbamic nitrogen in the piperazine-based compounds **4e,f** led to the carboxylic (**4e**) and hydroxamic (**4f**) acids displaying inhibitory activities in the micromolar and nanomolar range, respectively. The enzymatic assays of this first set of derivatives highlighted a dual FAAH-HDAC6 inhibitory profile only for the hydroxamic acid-bearing compounds **4c,f**, which display IC₅₀ values against HDAC6 in the micromolar range. The presence of the ZBG at position 3 of the pyrrole ring, allowed the bidentate chelation of the zinc ion and the formation of a π - π stacking between the phenyl-pyrrole moiety and Phe620 and Phe680, as depicted in Figure 3. Interestingly, compound **4d**, characterized by the ZBG at position 2 of the pyrrole ring, resulted completely inactive against this target, probably due to its unfavorable geometry that hampers the accommodation within the narrow binding pocket.

In the second set of compounds (**4g–j**), we explored the substitution of the distal phenyl ring of the lateral chain. While the introduction of the hydroxamic acid led to potent HDAC6is (**4h–j**), the inhibition of FAAH resulted in variable. Indeed, appending the

ZBG on the phenyl ring of a piperazine-bearing lateral chain led to the totally inactive FAAH inhibitors **4i** and **4j**. On the other hand, compound **4h** displayed a balanced submicromolar inhibitory profile against both targets (FAAH IC₅₀ = 297 ± 17 nM, HDAC6 IC₅₀ = 370 ± 23 nM, Table 1). As shown in Figure 4a, the docking pose of the phenyl-pyrrole core of compound **4h** mimics the interactions of reference compound **1**; while the presence on the distal phenyl ring of the polar hydroxamic acid, which is involved in an H-bond with Thr377, leads to a more elongated conformation of the lateral chain within the ACB pocket. As regards HDAC6 inhibition, the introduction of the ZBG on the phenyl ring of compound **4h** lateral chain determines an inverted binding mode on HDAC6 compared to **4c,f**. In this case, the hydroxamic acid, which is appended to a slender and more flexible phenyl-hexyl chain, can more easily reach the zinc ion at the bottom of the catalytic pocket (Figure 4b).

As a proof of concept, the replacement of the hydroxamic acid with a methyl ester moiety, as in compound **4g**, totally suppressed the HDAC6 inhibitory profile. On the other hand, this structural modification proved to be beneficial for FAAH inhibition (IC₅₀ = 31 ± 2 nM, Table 1). The calculation of the binding free energy of compounds **4g** and **4h** to FAAH clearly shows a detrimental effect of the highly polar and deprotonated hydroxamate group within the hydrophobic ACB pocket, when compared to the methyl ester moiety under the assay conditions (pH = 9) (Figure 5). Indeed, this is in line with previously reported evidence, highlighting the hydrophobic nature of the active site.^[48]



SCHEME 5 Synthesis of the second set of title compounds (**4g–j**). Reagents and conditions: (a) 4-nitrophenyl chloroformate, dry TEA, dry DCM, and phenol **23e**, 0°C, 3 h, then amine **14a–d**, 25°C, 3 h, 27%–54%; (b) H₂, Pd/C, MeOH/EtOAc, 25°C, 2 h, 39%; (c) HCOOH (88% in water), 15 min, 53%–80% (for **4i,j**).

2.2.3 | Assessment of neuroprotective and antioxidant effects and toxicity evaluation

In the context of neurodegeneration, reactive oxygen species (ROS) play a pivotal role in cell homeostasis. An imbalanced production or an ineffective disposal of ROS can trigger damaging signaling cascades, often leading to impaired functions and cell death.^[49] Therefore, we selected the most promising MTDLs (**4f,h**) and the selective FAAHi **4a** to investigate their efficacy in acute models of *tert*-butyl hydroperoxide (TBHP)-induced oxidative stress in both 1321N1 *human* astrocytes and SH-SY5Y *human* neuronal cell lines.

On 1321N1 cells, compounds **4h** and **4f**, the first-in-class FAAH-HDAC MTDLs, reduced TBHP-stimulated ROS production in a concentration-dependent manner and showed a greater effect compared to the reference antioxidant *N*-acetylcysteine (NAC) (Figure 6a). In contrast, compound **4a**, which solely inhibits FAAH, did not show any significant effect on ROS levels, highlighting the value of the polypharmacological approach. When tested on

neuron-like cells SH-SY5Y, compounds **4h** and **4f** also exhibited an effect on reducing TBHP-stimulated ROS production, although to a lesser extent than NAC, while compound **4a** remained ineffective (Figure 6b). The corresponding IC₅₀ values are reported in Supporting Information: Table S1. Furthermore, the toxicity profile of the newly developed compounds was evaluated on the same cell lines. Compounds **4h** and **4f** showed no significant cytotoxicity at the concentrations used, indicating their safety within the tested range, both in 1321N1 astrocytes (Figure 6c) and SH-SY5Y neuron-like cells (Figure 6d). Compound **4a** significantly reduced 1321N1 and SH-SY5Y cell viability although only at the concentration of 30 μM. Astrocytes serve a crucial function in protecting the CNS from oxidative damage and glutamate-induced toxicity.^[50,51] Given their vital role, we examined the potential of newly synthesized compounds to mitigate the damage induced by TBHP or glutamate in 1321N1 cells. Compounds **4h**, **4f**, and **4a** significantly prevented a decrease in cell viability triggered by 1 mM TBHP (Figure 6e). Furthermore, the multitarget FAAH-HDACis **4h** and **4f**, but not the selective FAAHi **4a** (tested at 10 μM),

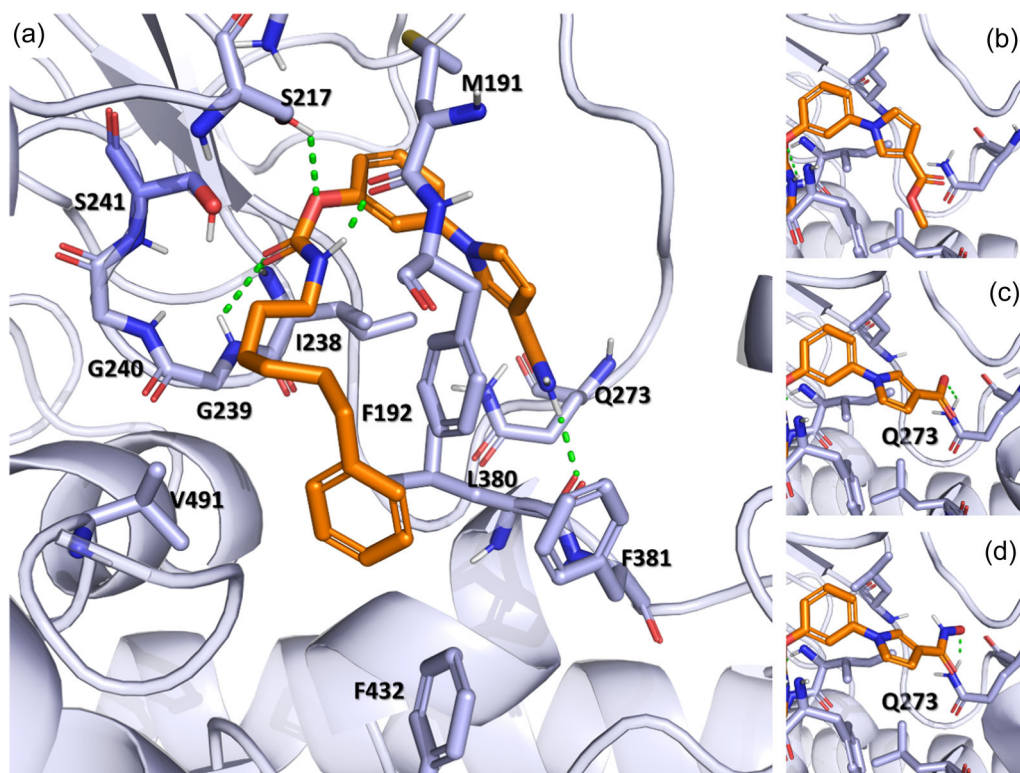


FIGURE 2 Docking pose of reference compound 1 within FAAH binding pocket (a). Details of the docking poses of the phenyl-pyrrole moiety of compounds 4a (b), 4b (c), and 4c (d). FAAH enzyme is represented as light blue cartoons and sticks, while the docked compounds are depicted as orange sticks; H-bonds between the ligands and the enzymes are displayed as green dashed lines.

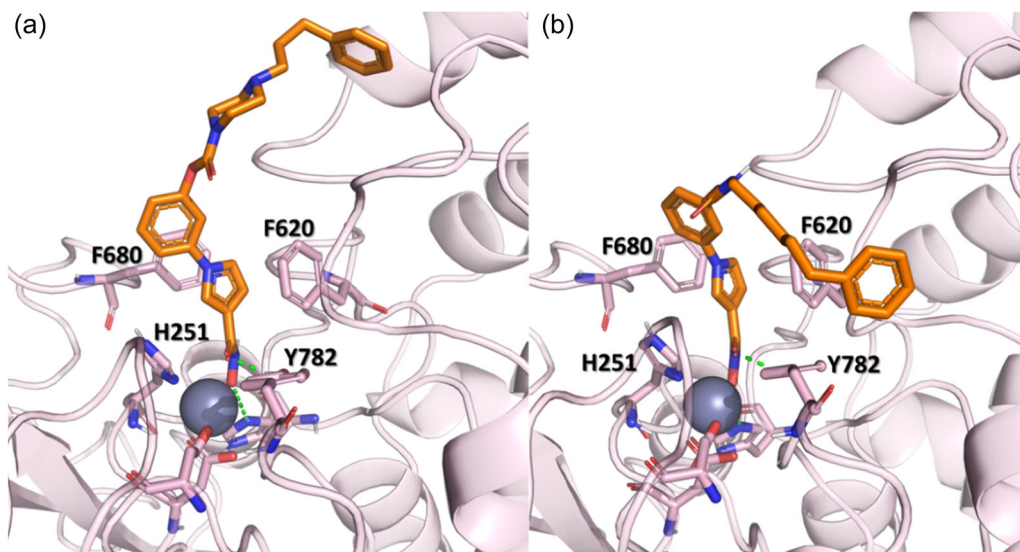


FIGURE 3 Docking pose of compounds 4c (a) and 4f (b) within histone deacetylase (HDAC) 6 binding pocket. HDAC6 enzyme is represented as light-pink cartoons and sticks, while the docked compounds are represented as orange sticks; Zn^{2+} ion is depicted as a gray sphere and H-bonds between the ligands and the enzymes are displayed as green dashed lines.

counteracted the toxic effects of 200 mM glutamate (Figure 6f). These findings suggest an enhanced oxidative stress resistance and ability for glutamate clearance by astrocytes, emphasizing the potential therapeutic role of these compounds in protecting the CNS.

3 | CONCLUSION

In the framework of polypharmacology and MTDL development for tackling CNS diseases, the simultaneous modulation of the ECS and epigenetic machinery had never been investigated. As a matter of

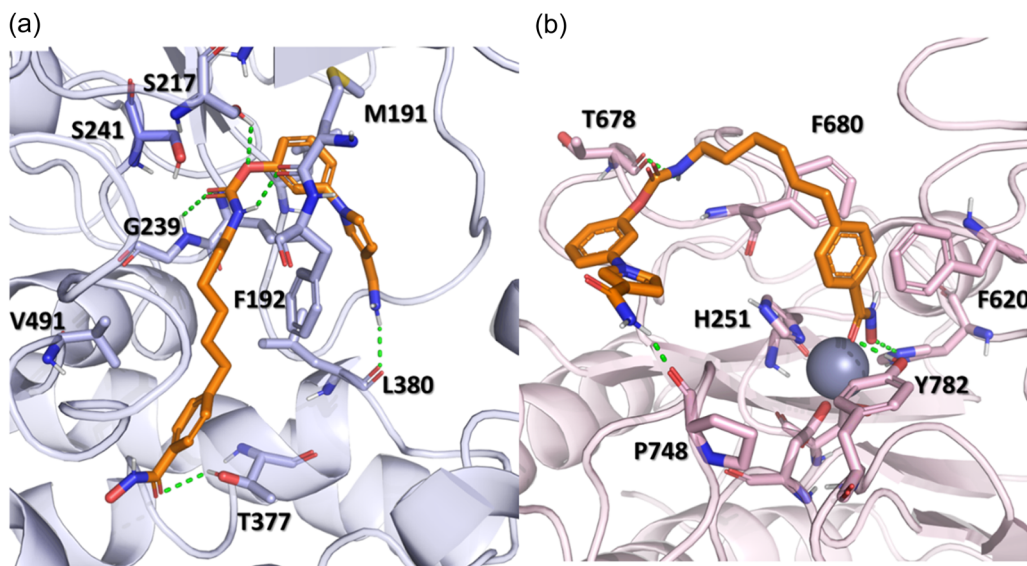


FIGURE 4 Docking pose of compound 4h within FAAH (a) and HDAC6 (b) binding pockets.

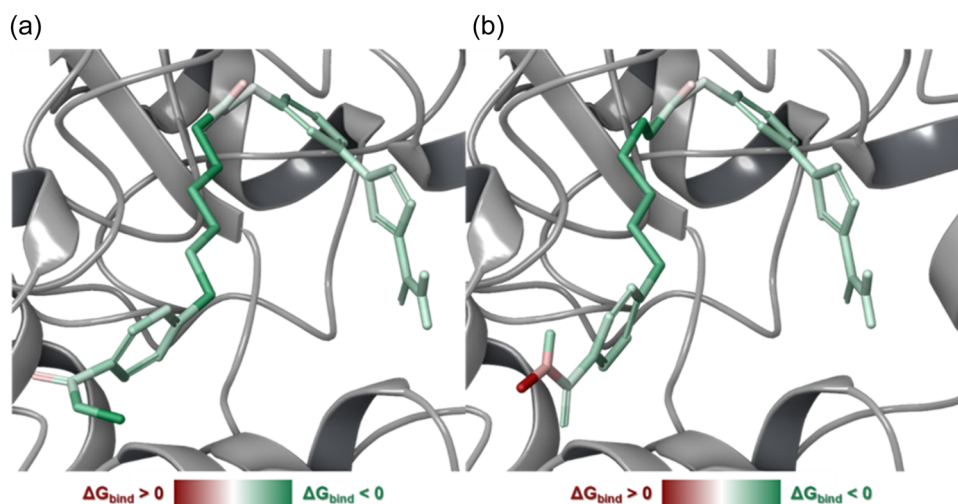


FIGURE 5 Prime energy visualization of the atomic contribution to the binding free energy of compounds 4g (a) and 4h (b) to fatty acid amide hydrolase. The green color represents the beneficial contribution to the binding, while the red color represents a detrimental contribution.

fact, FAAH-HDAC was an unprecedented combination of biological targets to date. Given the ubiquitous nature of both networks and their compelling role in several pathological conditions, we tackled the issue of developing potentially superior neuroprotective agents by combining the known neuroprotective effects of FAAHs with the recently evidenced therapeutic benefits of HDACs in oxidative stress-related CNS diseases.

Our work led us to the identification of the first-in-class FAAH-HDAC MTDLs, obtained by merging the pharmacophoric elements of FAAHs **1,2** with the ones of HDACi **3**, sharing a common 1-phenylpyrrole scaffold. To explore which structural decoration on our 1-phenylpyrrole-based FAAHs ensued effective engagement of the HDAC enzymes, two series of hybrid compounds (**4a-f** and **4g-j**) were designed and synthesized. Molecular docking experiments on

*h*FAAH and *h*HDAC6 elucidated the different binding modes of the two sets of derivatives inside the catalytic pocket of both targets and highlighted that the highly polar hydroxamic moiety has a detrimental effect on FAAH inhibition, despite being essential for HDAC engagement. Following the initial enzymatic assays, the best-performing compounds were subjected to a panel of preliminary ADME studies, evaluating their solubility and chemical stability at pH 3.0 and 7.4 and predicting some relevant pharmacokinetic parameters (e.g., blood-brain barrier permeability, cytochrome P450 induction, cell permeability). Compounds **4c**, **4f**, and **4h** were then tested in different TBHP-induced oxidative stress cellular models to assess their neuroprotective effect. Hit compound **4h** not only showed a well-balanced nanomolar inhibitory activity against the selected targets (*h*FAAH $IC_{50} = 297 \pm 17$ nM, *h*HDAC6 $IC_{50} = 370 \pm 23$ nM)

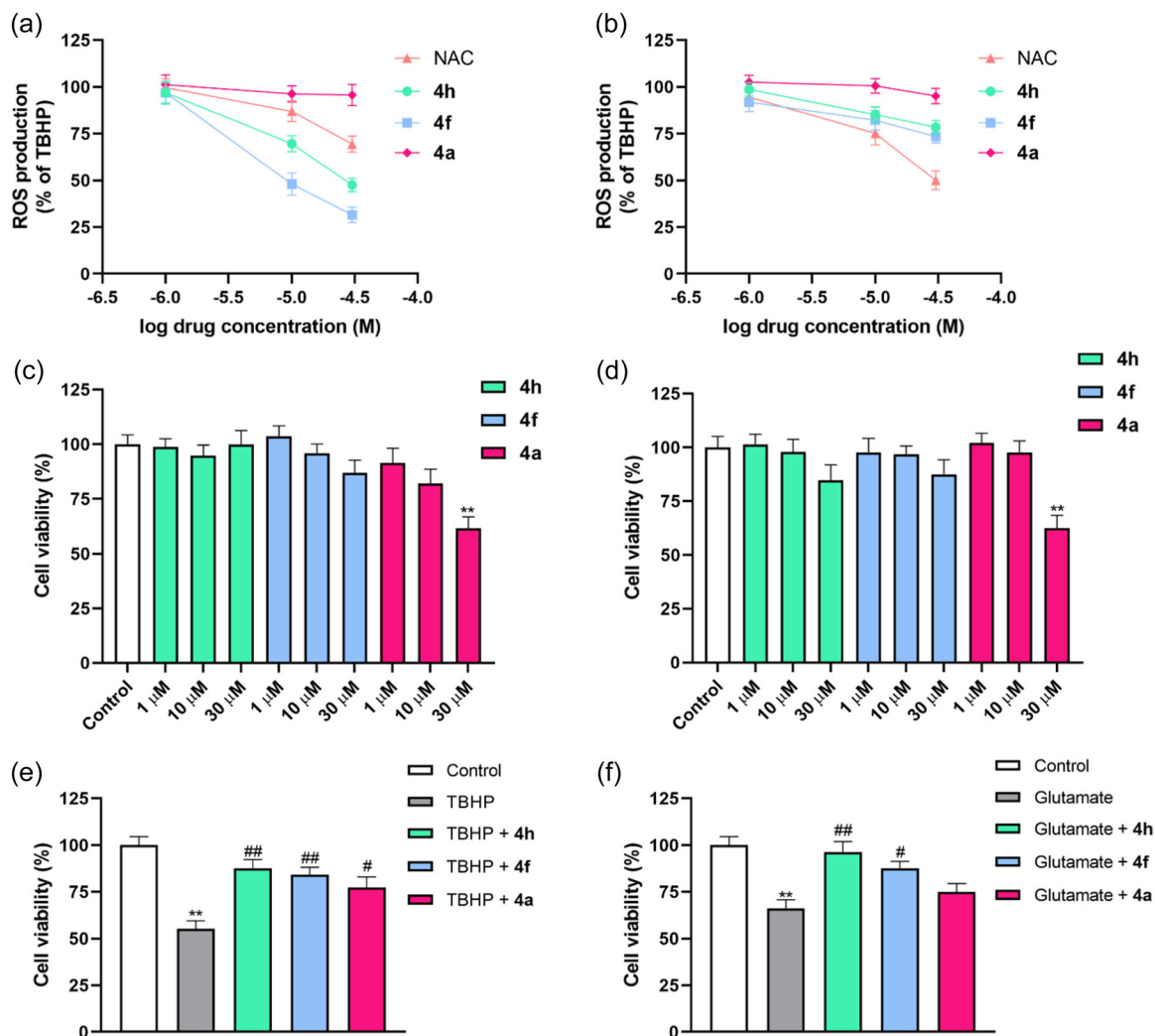


FIGURE 6 Evaluation of the antioxidant and neuroprotective profile of the first-in-class FAAH-HDAC MTDLs **4h,f** in comparison to the selective FAAHi **4a** and NAC. The effect of newly developed compounds **4h**, **4f**, and **4a** in comparison to NAC on the reduction of ROS production induced by 50 μ M TBHP was evaluated in 1321N1 *human* astrocytes (a) and in SH-SY5Y *human* neuronal (b) cell lines. Cytotoxicity was assessed after a 24-h incubation with the new compounds, in both 1321N1 (c) and SH-SY5Y (d) cells. The ability of the new compounds to protect 1321N1 cells from damage induced by 24 h of 1 mM TBHP (e) or 200 mM glutamate (f) was evaluated by preincubating the compounds (10 μ M) for 24 h before exposure to the noxious stimuli. ** $p < 0.01$ versus control; # $p < 0.05$ versus TBHP or glutamate; ## $p < 0.01$ versus TBHP or glutamate.

but also outperformed NAC on 1321N1 astrocytes, showing no significant cytotoxicity. Additional tests were conducted to determine the efficacy of the newly synthesized MTDLs **4f,h** in mitigating glutamate-induced toxicity in 1321N1 cells. Taken together these preliminary studies suggest that these compounds possess significant therapeutic potential, as they have demonstrated remarkable capabilities in mitigating TBHP or glutamate-induced harm, successfully preventing a reduction in cell viability in the same cell line. Considerable insight has been gained regarding the concurrent targeting of these two biological systems and our investigations into this area are still ongoing, without overlooking the ADME properties optimization. The findings disclosed here may potentially pave the way for the development of additional libraries of MTDLs targeting

the ECS and epigenetic enzymes, which could represent an innovative pharmacological expedient for the treatment of oxidative stress-related CNS diseases.

4 | EXPERIMENTAL

4.1 | Chemistry

4.1.1 | General

All reagents were purchased from commercial suppliers and used without further purification. All moisture-sensitive reactions were

performed under a nitrogen atmosphere using oven-dried glassware and dry solvents. Dry tetrahydrofuran (THF) was freshly distilled from sodium/benzophenone, while dichloromethane (DCM) and *N,N*-dimethylformamide (DMF) were freshly distilled from calcium hydride and stored under argon atmosphere. Flash column chromatography was carried out on silica gel (Merck: Kieselgel 60, particle size 0.040–0.063 mm). Reactions' progression was monitored by thin-layer chromatography (TLC), carried out using glass-backed plates coated with Merck Kieselgel 60 GF254. Plates were visualized under UV light (at 254 nm) or by staining with potassium permanganate, ninhydrin, or cerium ammonium molybdate followed by heating. ¹H NMR and ¹³C NMR spectra were recorded on a Varian 300 MHz spectrometer using the residual signal of the deuterated solvent as an internal standard. Coupling constants (*J*) are given in hertz (Hz). Splitting patterns are described as singlet (s), doublet (d), triplet (t), quartet (q), multiplet (m), and broad (br); the value of chemical shifts (δ) is given in parts per million (ppm). Mass spectra were recorded utilizing an electron spray ionization (ESI) Agilent 1100 Series LC/MSD spectrometer. ESI-HRMS spectra were acquired by a linear ion-trap-Orbitrap hybrid mass spectrometer (LTQ Orbitrap XL) (Thermo Fisher Scientific) operating in positive electrospray ionization mode. Data were collected and analyzed using the Xcalibur 2.2 software provided by the manufacturer and the spectra are available in the Supporting Information. Yields refer to purified products and are not optimized. Target compounds were analyzed by HPLC analysis to confirm purity >95%.

The InChI codes of the investigated compounds, together with some biological activity data, are provided as Supporting Information.

4.1.2 | Procedures for the synthesis of intermediates and target products

General procedure A: Synthesis of key carbamate intermediates and target compounds (4a,g, 29a–c, 30a,b, and 31a–c)

To a solution of phenols **23a–e** (1 eq) in dry DCM under N₂ atmosphere at 0°C, dry TEA (3 eq) and 4-nitrophenyl chloroformate (1.5 eq) were added. The reaction mixture was stirred for 3 h at 0°C. Subsequently, a solution of the amine **14a–f** (1.5 eq) in dry DCM was added and the reaction was stirred for 3 h at 25°C. The reaction mixture was quenched with water and extracted with DCM (3 × 10 mL). The combined organic layers were dried over sodium sulfate, filtered, and concentrated under reduced pressure. The crude was purified by means of chromatography on silica gel, eluting as indicated for each intermediate.

General procedure B: Deprotection of O-benzyl-protected carboxylic and hydroxamic acids (4b–f, 4h)

To a solution of O-benzyl-protected hydroxamic acids **29a–c**, **30a,b**, or **31a** in EtOAc/MeOH (2:1) under N₂ atmosphere at 25°C, Pd/C 10% was added. The reaction mixture was stirred at 25°C under an H₂ atmosphere for 2 h. The reaction mixture was filtered, and the filtrate was evaporated under reduced pressure. The crude was

purified by means of chromatography on silica gel, eluting as indicated for each intermediate.

General procedure C: Deprotection of O-THP-protected hydroxamic acids (4i,j)

O-THP-protected hydroxamic acids **31b,c** were treated with 88% aqueous HCOOH. The reaction mixture was stirred at 25°C for 15 min. Then, the solvent was removed under reduced pressure. The crude was purified by means of chromatography on silica gel, eluting as indicated for each intermediate.

[4-(Methoxycarbonyl)benzyl]triphenylphosphonium bromide (6)

To a solution of methyl 4-(bromomethyl)benzoate **5** (2000 mg, 8.73 mmol) in dry toluene (17.5 mL), triphenylphosphine (2290 mg, 8.73 mmol) was added. The reaction mixture was refluxed for 16 h. After cooling to 25°C, the reaction mixture was filtered. The solid residue was washed with toluene and the residual solvent was removed under vacuum. The crude was used in the next step without any further purification (99% yield, white solid). Spectroscopic data are in agreement with those reported.^[52]

2-(5-Hydroxypentyl)isoindoline-1,3-dione (8)

To a solution of 5-aminopentan-1-ol **7** (1000 mg, 9.69 mmol) in dry toluene (9.7 mL), phthalic anhydride (1436 mg, 9.69 mmol) was added. The reaction mixture was refluxed for 24 h. After cooling to 25°C, the solvent was removed under vacuum. The crude was taken up with diethyl ether and filtered. The solution was washed with 1 N HCl (3 × 10 mL). Then, the organic layers were dried over sodium sulfate, filtered, and concentrated. The crude was used in the next step without any further purification (80% yield, yellow oil). ¹H NMR (300 MHz, CDCl₃) δ 7.80–7.54 (m, 4H), 3.59 (dt, *J* = 13.0, 6.8 Hz, 4H), 1.74–1.47 (m, 4H), 1.42–1.25 (m, 2H).

5-(1,3-Dioxoisindolin-2-yl)pentanal (9)

To a solution of **8** (200 mg, 0.86 mmol) in dry DCM (2.7 mL) at 0°C, TCICA (209 mg, 0.90 mmol) and TEMPO (1.34 mg, 0.01 mmol) were added. The mixture was stirred at 0°C for 15 min. The reaction mixture was then filtered through celite and washed with DCM. The collected organic layers were washed with a saturated solution of NaHCO₃ and 1 N HCl, then dried over sodium sulfate, filtered, and concentrated. The crude was used in the next step without any further purification (99% yield, yellow oil). ¹H NMR (300 MHz, (CD₃)₂CO) δ 9.72 (s, 1H), 7.83–7.75 (m, 4H), 3.70–3.57 (m, 2H), 2.55–2.46 (m, 2H), 1.80–1.55 (m, 4H).

Methyl (E/Z)-4-[6-(1,3-dioxoisindolin-2-yl)hex-1-en-1-yl] benzoate (10)

To a solution of **6** (841 mg, 1.71 mmol) in dry THF (7 mL) at 0°C, KHMDS (0.5 M solution in toluene, 2568 μ L, 1.28 mmol) was added. The reaction mixture was stirred at 0°C for 30 min. Then, a solution of **9** (396 mg, 1.7 mmol) in dry THF (4 mL) was added at 0°C. The reaction mixture was stirred for 16 h at 25°C, under an N₂ atmosphere. The reaction mixture was quenched with a saturated

solution of NH_4Cl and extracted with EtOAc (2×10 mL). The collected organic layers were dried over sodium sulfate, filtered, and concentrated. The crude was purified by column chromatography on silica gel (PE/EtOAc from 7:1 to 3:1) to afford the title compound as a white solid (83% yield). ^1H NMR (300 MHz, CDCl_3) δ 7.93–7.81 (m, 2H), 7.78–7.69 (m, 2H), 7.65–7.58 (m, 2H), 7.32–7.16 (m, 2H), 6.39–6.17 (m, 2H), 3.82 (d, $J = 3.6$ Hz, 3H), 3.69–3.54 (m, 2H), 2.35–2.13 (m, 2H), 1.75–1.57 (m, 2H), 1.54–1.39 (m, 2H).

Methyl 4-[6-(1,3-dioxoisindolin-2-yl)hexyl]benzoate (11)

To a solution of **10** (515 mg, 1.42 mmol) in EtOAc/MeOH 2:1 (45 mL), Pd/C 10% (0.14 mol) was added. The reaction mixture was stirred under an H_2 atmosphere for 1 h. The reaction mixture was filtered and the filtrate was evaporated under reduced pressure. The crude was used in the next step without any further purification (90% yield, white solid). ^1H NMR (300 MHz, CDCl_3) δ 7.91 (d, $J = 8.1$ Hz, 2H), 7.86–7.75 (m, 2H), 7.73–7.61 (m, 2H), 7.19 (d, $J = 8.1$ Hz, 2H), 3.87 (s, 3H), 3.65 (t, $i = 7.0$ Hz, 2H), 2.62 (t, $J = 7.6, 7.2$ Hz, 2H), 1.63 (dt, $J = 14.1, 6.5$ Hz, 4H), 1.43–1.27 (m, 4H).

Methyl 4-(6-aminohexyl)benzoate (14a)

To a solution of **11** (63 mg, 0.17 mmol) in EtOH (0.9 mL), hydrazine monohydrate (33 μL , 0.69 mmol) was added. The solution was refluxed for 1 h until the appearance of a white precipitate, which was removed by filtration. The filtrate was concentrated under reduced pressure. The crude was taken up with water, treated with 1 N HCl, and extracted with DCM (3×10 mL). The combined aqueous layers were treated with 1 NaOH to reach pH = 8 and extracted with DCM (3×5 mL). The organic layer was dried over dry sodium sulfate, filtered, and concentrated. The crude was used in the next step without any further purification (72% yield, pale-yellow oil). ^1H NMR (300 MHz, CDCl_3) δ 7.96–7.90 (m, 2H), 7.24–7.18 (m, 2H), 3.88 (s, 3H), 2.94 (br, 2H), 2.78–2.67 (m, 2H), 2.67–2.58 (m, 2H), 1.69–1.54 (m, 2H), 1.54–1.41 (m, 2H), 1.38–1.28 (m, 4H).

4-[6-(1,3-Dioxoisindolin-2-yl)hexyl]benzoic acid (12)

To a solution of **11** (313 mg, 0.86 mmol) in THF (18 mL), a 0.1 NaOH aqueous solution (137 mg, 3.43 mmol, 18 mL) was added. The reaction mixture was stirred for 16 h at 25°C. The reaction mixture was quenched with 6 N HCl and extracted with EtOAc (3×20 mL). The organic layers were dried over sodium sulfate, filtered, and concentrated. The crude was used in the next step without any further purification (99% yield, white solid). ^1H NMR (300 MHz, CD_3OD) δ 7.97–7.88 (m, 3H), 7.62–7.46 (m, 2H), 7.40 (dd, $J = 7.4, 1.4$ Hz, 1H), 7.29 (d, $J = 8.2$ Hz, 2H), 3.33–3.28 (m, 2H), 2.69 (t, $J = 8.0, 7.6$ Hz, 2H), 1.75–1.53 (m, 4H), 1.49–1.34 (m, 4H).

N-(Benzyloxy)-4-[6-(1,3-dioxoisindolin-2-yl)hexyl]benzamide (13)

To a solution of **12** (76 mg, 0.22 mmol) in dry THF (3 mL), thionyl chloride (224 μL , 3.07 mmol) was added dropwise. The reaction mixture was refluxed for 2 h under an N_2 atmosphere. After cooling to 25°C, the solvent was removed, the solid residue was dissolved in DCM and then, the solvent was removed under vacuum. This

procedure was repeated twice. The obtained solid was dissolved in dry DCM (2 mL) and then, DIPEA (79 μL , 0.45 mmol) and *O*-benzylhydroxylamine hydrochloride (27 mg, 0.17 mmol) were added. The reaction mixture was stirred at 25°C, under an N_2 atmosphere for 16 h. A saturated solution of NH_4Cl was added and the mixture was extracted with DCM (3×10 mL). The collected organic layers were dried over sodium sulfate, filtered, and concentrated. The crude was purified by column chromatography on silica gel (PE/EtOAc from 3:1 to 1:1) to afford the title compound as a white solid (29% yield). ^1H NMR (300 MHz, $(\text{CD}_3)_2\text{CO}$) δ 10.73 (s, 1H), 7.84 (s, 4H), 7.76–7.65 (m, 2H), 7.48 (dd, $J = 7.7, 1.7$ Hz, 2H), 7.42–7.33 (m, 2H), 7.30–7.25 (m, 2H), 5.00 (s, 2H), 3.64 (t, $J = 7.1$ Hz, 2H), 2.70–2.60 (m, 2H), 1.72–1.56 (m, 4H), 1.43–1.34 (m, 4H).

4-(6-Aminohexyl)-N-(benzyloxy)benzamide (14b)

The title compound was prepared according to the procedure used for **14a** starting from **13** (74 mg, 0.16 mmol) and hydrazine monohydrate (31 μL , 0.65 mmol). The crude was used in the next step without any further purification (99% yield, pale-yellow oil). ^1H NMR (300 MHz, CD_3OD) δ 8.19 (dd, $J = 6.0, 3.3$ Hz, 1H), 7.78 (dd, $J = 6.0, 3.3$ Hz, 1H), 7.62 (d, $J = 8.2$ Hz, 2H), 7.48 (dd, $J = 7.4, 2.2$ Hz, 1H), 7.37 (dd, $J = 6.4, 1.6$ Hz, 2H), 7.26 (d, $J = 8.2$ Hz, 2H), 4.96 (s, 2H), 2.85–2.77 (m, 2H), 2.66 (t, $J = 7.6$ Hz, 2H), 1.71–1.47 (m, 4H), 1.47–1.28 (m, 4H).

Ethyl 4-(3-oxopropyl)benzoate (16)

To a suspension of NaHCO_3 (599 mg, 7.14 mmol), TBAB (460 mg, 1.43 mmol), and $\text{Pd}(\text{OAc})_2$ (12.8 mg, 0.06 mmol) in dry DMF (1.4 mL), a solution of ethyl 4-iodobenzoate **15** (788 mg, 2.85 mmol) and allyl alcohol (292 μL , 4.28 mmol) in dry DMF (1 mL) was added. The reaction mixture was heated at 80°C for 3 h. Then, the reaction mixture was cooled to 25°C and filtered through a celite pad, washing with EtOAc. The filtrate was treated with water and extracted with EtOAc (2×10 mL). Then, the collected organic phase was washed with brine (2×10 mL). The crude was purified by column chromatography on silica gel (5:1 petroleum ether/ Et_2O) to afford the title compound as a clear liquid (59%). ESI-MS m/z : 205.0 $[\text{M}-\text{H}]^-$. ^1H NMR (300 MHz, CD_3OD) δ 9.72 (s, 1H), 7.90 (d, $J = 8.3$ Hz, 2H), 7.30 (d, $J = 8.2$ Hz, 2H), 4.31 (q, $J = 7.1$ Hz, 2H), 2.95 (t, $J = 7.4$ Hz, 2H), 2.78 (t, $J = 7.4$ Hz, 2H), 1.35 (t, $J = 7.1$ Hz, 3H).

Benzyl 4-[3-[4-(ethoxycarbonyl)phenyl]propyl]piperazine-1-carboxylate (17)

To a solution of **16** (100 mg, 0.49 mmol) and 1-Cbz-piperazine (107 mg, 0.49 mmol) in dry MeOH (1.6 mL) cooled at 0°C, NaBH_3CN (37 mg, 0.58 mmol) was added. The mixture was stirred at 0°C for 1 h and then at 25°C for 16 h. After quenching the reaction mixture with water, the organic solvent was removed under reduced pressure. The residue was diluted with water and extracted with DCM (3×10 mL). The collected organic layers were washed with a saturated solution of NaHSO_3 (2×10 mL). The crude was used in the next step without any further purification (99% yield, clear oil). ESI-MS m/z : 411.2 $[\text{M}+\text{H}]^+$; 433.2 $[\text{M}+\text{Na}]^+$. ^1H NMR (300 MHz, CD_3OD) δ 7.91 (d,

$J = 8.2$ Hz, 2H), 7.37–7.16 (m, 7H), 5.09 (d, $J = 4.2$ Hz, 2H), 4.30 (q, $J = 7.2$ Hz, 2H), 2H), 3.65–3.40 (m, 4H), 2.86–2.73 (m, 1H), 2.66 (t, $J = 7.6$ Hz, 2H), 2.43–2.30 (m, 4H), 2.11–1.99 (m, 1H), 1.88–1.72 (m, 2H), 1.39–1.28 (m, 3H).

4-(3-{4-[(Benzyloxy)carbonyl]piperazin-1-yl}propyl)benzoic acid (18)

The title compound was prepared according to the procedure used for **12** starting from compound **17** (198 mg, 0.48 mmol) and 0.1 N NaOH solution (77 mg, 1.929 mmol). The crude was used in the next step without any further purification (88% yield, pale-yellow oil). ESI-MS: 383.2 [M+H]⁺. ¹H NMR (300 MHz, CD₃OD) δ 7.94 (d, $J = 7.9$ Hz, 2H), 7.41–7.24 (m, 7H), 5.11 (d, $J = 5.5$ Hz, 2H), 3.80–3.74 (m, 2H), 3.60–3.50 (m, 1H), 3.29 (s, 4H), 3.15 (t, $J = 8.2$ Hz, 1H), 2.76 (t, $J = 7.7$ Hz, 2H), 2.12 (s, 4H).

Benzyl 4-[3-(4-[(tetrahydro-2H-pyran-2-yl)oxy]carbamoyl)phenyl)propyl]piperazine-1-carboxylate (19)

To a solution of **18** (162 mg, 0.42 mmol) in a 7:1 mixture of dry DCM and dry DMF (3.3 mL), *O*-(tetrahydro-2H-pyran-2-yl)hydroxylamine (50 mg, 0.42 mmol) and EDC-HCl (97 mg, 0.51 mmol) were added at 25°C. The reaction mixture was stirred at 25°C for 18 h. The reaction mixture was quenched with a saturated solution of NH₄Cl, and DCM was removed under reduced pressure. The residue was then extracted with EtOAc (3 × 10 mL). The collected organic layers were washed with a saturated solution of NH₄Cl (2 × 10 mL) and brine (1 × 10 mL). The crude was purified by column chromatography on silica gel (EtOAc) to afford the title compound as a clear liquid (41%). ESI-MS: 482.2 [M+H]⁺; 504.2 [M+Na]⁺. ¹H NMR (300 MHz, (CD₃)₂CO) δ 10.70 (s, 1H), 7.76 (d, $J = 8.1$ Hz, 2H), 7.44–7.26 (m, 7H), 5.14–5.05 (m, 3H), 4.15–4.01 (m, 1H), 3.62–3.41 (m, 5H), 2.70 (t, $J = 7.6$ Hz, 2H), 2.40–2.27 (m, 6H), 1.89–1.69 (m, 4H), 1.60–1.47 (m, 4H).

4-[3-(Piperazin-1-yl)propyl]-N-[(tetrahydro-2H-pyran-2-yl)oxy]benzamide (14c)

To a solution of compound **19** in MeOH under an N₂ atmosphere at 25°C, Pd/C 10% was added. The reaction mixture was stirred at 25°C under an H₂ atmosphere for 3 h. The reaction mixture was filtered and the filtrate was evaporated under reduced pressure. The crude was purified by column chromatography on silica gel (DCM/MeOH 10:1 to DCM/MeOH/NH₄OH 10:1:0.1) to afford the title compound as a pale-yellow oil (58% yield). ESI-MS m/z : 348.2 [M+H]⁺; 370.1 [M+Na]⁺; 386.1 [M+K]⁺. ¹H NMR (300 MHz, CD₃OD) δ 7.79 (d, $J = 8.3$ Hz, 1H), 7.70 (d, $J = 8.2$ Hz, 2H), 7.29 (d, $J = 8.2$ Hz, 2H), 5.04 (s, 1H), 4.19–4.05 (m, 1H), 3.68–3.55 (m, 1H), 2.83 (t, $J = 5.0$ Hz, 4H), 2.76–2.59 (m, 2H), 2.46–2.41 (m, 4H), 2.41–2.30 (m, 2H), 1.95–1.74 (m, 5H), 1.73–1.53 (m, 3H).

4-(Bromomethyl)-N-[(tetrahydro-2H-pyran-2-yl)oxy]benzamide (21)

The title compound was prepared according to the procedure used for **19** starting from 4-(bromomethyl)benzoic acid **20** (100 mg, 0.465 mmol), *O*-(tetrahydro-2H-pyran-2-yl)hydroxylamine (55 mg, 0.465 mmol), and EDC-HCl (107 mg, 0.558 mmol). The crude was purified by column chromatography on silica gel (1:1 petroleum

ether/EtOAc) to afford the title compound as an amorphous white solid (99% yield). ¹H NMR (300 MHz, CDCl₃) δ 9.50 (s, 1H), 7.73 (d, $J = 8.1$ Hz, 2H), 7.38 (d, $J = 8.1$ Hz, 2H), 5.04 (s, 1H), 4.56 (s, 2H), 3.98 (t, $J = 9.9$ Hz, 1H), 3.58 (m, 1H), 1.97–1.68 (m, 3H), 1.73–1.41 (m, 3H).

4-(Piperazin-1-ylmethyl)-N-[(tetrahydro-2H-pyran-2-yl)oxy]benzamide (14d)

To a solution of piperazine (82 mg, 0.955 mmol) and K₂CO₃ (44 mg, 0.318 mmol) in dry THF (17 mL), heated at 65°C, compound **21** (100 mg, 0.318 mmol) was added. The reaction mixture was stirred at 65°C for 16 h. Then, the solvent was removed under reduced pressure. The crude was purified by column chromatography on silica gel (5:1 DCM/MeOH) to afford the title compound as an amorphous yellow waxy solid (99%). ESI-MS m/z : 320.2 [M+H]⁺; 342.1 [M+Na]⁺; 358.1 [M+K]⁺. ¹H NMR (300 MHz, CD₃OD) δ 7.76 (d, $J = 8.2$ Hz, 2H), 7.45 (d, $J = 8.1$ Hz, 2H), 5.04 (s, 1H), 4.12 (t, $J = 10.3$ Hz, 1H), 3.68–3.56 (m, 3H), 3.25–3.09 (m, 4H), 2.73–2.59 (m, 4H), 1.95–1.72 (m, 3H), 1.74–1.50 (m, 3H).

Methyl 1-(3-hydroxyphenyl)-1H-pyrrole-3-carboxylate (23a)

To a solution of **22** (203 mg, 1 mmol) in MeOH (5 mL), TMSCl (279 μ L, 2.2 mmol) was added at 0°C. The reaction mixture was allowed to reach 25°C and was stirred at 25°C for 14 h. Then, the solvent was removed under reduced pressure (89% yield, off-white solid). ESI-MS m/z : 216 [M-H]⁻. ¹H NMR (300 MHz, CDCl₃) δ 7.68 (s, 1H), 7.34–7.22 (m, 1H), 7.04–6.89 (m, 3H), 6.83 (d, $J = 7.6$ Hz, 1H), 6.72 (dd, $J = 2.7, 1.5$ Hz, 2H), 3.86 (s, 3H).

Benzyl 1-(3-hydroxyphenyl)-1H-pyrrole-3-carboxylate (23b)

To a solution of **22** (50 mg, 0.45 mmol) in dry DMF (2 mL), NaHCO₃ (101 mg, 0.54 mmol), and benzyl bromide (80 μ L, 0.68 mmol) were added. The reaction mixture was heated to 40°C and stirred for 16 h under an N₂ atmosphere. A saturated solution of NH₄Cl was added and the mixture was extracted with EtOAc (3 × 10 mL). The combined organic layers were washed with a saturated solution of NH₄Cl (1 × 10 mL) and brine (2 × 10 mL). The organic phase was dried over sodium sulfate, filtered, and concentrated. The crude was purified by column chromatography on silica gel (PE/EtOAc from 3:1 to 2:1) to afford the title compound as an amorphous off-white solid (36% yield). ¹H NMR (300 MHz, (CD₃)₂CO) δ 8.86 (s, 1H), 7.84 (t, $J = 2.0$ Hz, 1H), 7.52–7.39 (m, 1H), 7.44–7.18 (m, 5H), 7.12–7.01 (m, 2H), 6.85 (dd, $J = 8.8, 2.2$ Hz, 1H), 6.72 (dd, $J = 3.1, 1.6$ Hz, 1H), 5.29 (s, 2H).

1-(3-Hydroxyphenyl)-1H-pyrrole-2-carbaldehyde (25a)

To a solution of oxalyl chloride (348 μ L, 4.05 mmol) in dry DCM (22.5 mL), under an N₂ atmosphere, a solution of dry DMF (314 μ L, 4.05 mmol) in dry DCM (2.0 mL) was added dropwise, at 0°C. The reaction mixture was stirred for 30 min under an N₂ atmosphere, at 0°C. Then, a solution of 3-(1H-pyrrol-1-yl)phenol **24** (461 mg, 2.90 mmol) in dry DCM (2.4 mL) was added at once. The reaction mixture was refluxed for 3 h. Then, the solvent was removed. The crude was dissolved in 1 N NaOH (10.5 mL) and stirred at 25°C for 16 h. The reaction mixture was quenched with 1 N HCl up to pH 5

and diluted with EtOAc. It was then extracted with EtOAc (3 × 10 mL). The organic layer was dried over sodium sulfate, filtered, and concentrated. The crude was purified by column chromatography on silica gel (PE/EtOAc from 10:1 to 3:1) to afford the title compound as a yellow solid (62% yield). ¹H NMR (300 MHz, (CD₃)₂CO) δ 9.59–9.57 (m, 1H), 8.84 (s, 1H), 7.35–7.28 (m, 1H), 7.28–7.23 (m, 1H), 7.17–7.09 (m, 1H), 6.97–6.93 (m, 1H), 6.93–6.86 (m, 2H), 6.44–6.38 (m, 1H).

1-[3-(Methoxymethoxy)phenyl]-1H-pyrrole-2-carbaldehyde (26a)

To a solution of **25a** (307 mg, 1.64 mmol) in dry DCM (15.1 mL), DIPEA (851 μL, 4.92 mmol) and MOM-Cl (374 μL, 4.92 mmol) were added. The reaction mixture was stirred at 0°C, under an N₂ atmosphere for 1 h. A saturated solution of NaHCO₃ was added and the mixture was extracted with DCM (3 × 10 mL). The organic layer was dried over sodium sulfate, filtered, and concentrated. The crude was purified by column chromatography on silica gel (PE/EtOAc from 6:1 to 4:1) to afford the title compound as an amorphous pale-yellow solid (96% yield). ¹H NMR (300 MHz, (CD₃)₂CO) δ 9.59 (s, 1H), 7.42 (t, *J* = 8.4 Hz, 1H), 7.30 (s, 1H), 7.19–7.10 (m, 3H), 7.10–7.04 (m, 1H), 6.43 (s, 1H), 5.27 (s, 2H), 3.45 (s, 3H).

1-[3-(Methoxymethoxy)phenyl]-1H-pyrrole-3-carbaldehyde (26b)

The title compound was prepared according to the procedure used for **26a** starting from **25b**^[14] (95 mg, 0.51 mmol), DIPEA (264 μL, 1.52 mmol) and MOM-Cl (116 μL, 1.52 mmol). The crude was purified by column chromatography on silica gel (PE/EtOAc from 6:1 to 3:1) to afford the title compound as an amorphous pale-yellow solid (84% yield). ¹H NMR (300 MHz, (CD₃)₂CO) δ 9.85 (s, 1H), 8.07–8.03 (m, 1H), 7.50–7.41 (m, 1H), 7.40–7.37 (m, 1H), 7.32–7.24 (m, 2H), 7.09–7.03 (m, 1H), 6.72 (dd, *J* = 3.1, 1.6 Hz, 1H), 5.30 (s, 2H), 3.46 (s, 3H).

1-[3-(Methoxymethoxy)phenyl]-1H-pyrrole-2-carboxylic acid (27a)

To a solution of **26a** (361 mg, 1.56 mmol) and 2-methyl-2-butene (2.16 mL, 20.29 mmol) in *tert*-butanol (12 mL), saturated solutions of NaClO₂ (0.69 mL, 5.78 mmol) and NaH₂PO₄ (1.10 mL, 7.81 mmol) were added. The reaction mixture was stirred for 16 h at 25°C. Then, it was quenched with a saturated solution of NH₄Cl and extracted with EtOAc (3 × 10 mL). The organic layer was dried over sodium sulfate, filtered, and concentrated. The crude was purified by column chromatography on silica gel (PE/EtOAc from 3:1 to EtOAc only) to afford the title compound as a colorless oil (91% yield). ¹H NMR (300 MHz, (CD₃)₂CO) δ 7.41–7.26 (m, 1H), 7.18–7.01 (m, 4H), 7.02–6.92 (m, 1H), 6.29 (s, 1H), 5.23 (s, 2H), 3.44 (s, 3H).

1-[3-(Methoxymethoxy)phenyl]-1H-pyrrole-3-carboxylic acid (27b)

The title compound was prepared according to the procedure used for **27a** starting from **26b** (365 mg, 1.58 mmol), 2-methyl-2-butene (2.18 mL, 20.51 mmol) and saturated solutions of NaClO₂ (1.02 mL, 8.84 mmol) and NaH₂PO₄ (1.70 mL, 11.84 mmol). The crude was purified by column chromatography on silica gel (PE/EtOAc from 4:1 to 1:1) to afford the title compound as a colorless oil (96% yield). ¹H

NMR (300 MHz, (CD₃)₂CO) δ 9.88 (br, 1H), 7.86–7.81 (m, 1H), 7.43 (t, *J* = 8.1 Hz, 1H), 7.32–7.22 (m, 3H), 7.05–6.99 (m, 1H), 6.69 (dd, *J* = 3.0, 1.6 Hz, 1H), 5.30 (s, 2H), 3.46 (s, 3H).

N-(Benzyloxy)-1-[3-(methoxymethoxy)phenyl]-1H-pyrrole-2-carboxamide (28a)

To a solution of **27a** (345 mg, 1.40 mmol) in dry THF (20 mL) at 25°C, TEA (777 μL, 5.59 mmol) was added. The suspension was stirred for 10 min, and then *O*-benzylhydroxylamine hydrochloride (223 mg, 1.40 mmol) and BOP-Cl (391 mg, 1.54 mmol) were added. The reaction mixture was stirred for 16 h under an N₂ atmosphere. A saturated solution of NH₄Cl was added and the reaction mixture was extracted with EtOAc (3 × 10 mL). Then, the combined organic layers were washed with a saturated solution of NaHCO₃. The organic phase was dried over sodium sulfate, filtered, and concentrated. The crude was purified by column chromatography on silica gel (PE/EtOAc from 8:1 to 1:1) to afford the title compound as an amorphous off-white solid (78% yield). ¹H NMR (300 MHz, (CD₃)₂CO) δ 10.43 (s, 1H), 7.49–7.26 (m, 6H), 7.14–7.00 (m, 3H), 6.95 (dt, *J* = 8.7, 1.1 Hz, 1H), 6.79–6.73 (m, 1H), 6.22 (dd, *J* = 3.7, 2.9 Hz, 1H), 5.24 (s, 2H), 4.93 (s, 2H), 3.45 (s, 3H).

N-(Benzyloxy)-1-[3-(methoxymethoxy)phenyl]-1H-pyrrole-3-carboxamide (28b)

The title compound was prepared according to the procedure used for **28a** starting from **27b** (52 mg, 0.21 mmol), TEA (117 μL, 0.84 mmol), *O*-benzylhydroxylamine hydrochloride (34 mg, 0.21 mmol), and BOP-Cl (59 mg, 0.23 mmol). The crude was purified by column chromatography on silica gel (PE/EtOAc from 3:1 to 1:1) to afford the title compound as an amorphous off-white solid (55% yield). ¹H NMR (300 MHz, (CD₃)₂CO) δ 10.37 (s, 1H), 7.82–7.78 (m, 1H), 7.52–7.32 (m, 6H), 7.30–7.26 (m, 1H), 7.25–7.15 (m, 2H), 7.05–6.96 (m, 1H), 6.70 (dd, *J* = 3.0, 1.7 Hz, 1H), 5.29 (s, 2H), 4.98 (s, 2H), 3.46 (s, 3H).

N-(Benzyloxy)-1-(3-hydroxyphenyl)-1H-pyrrole-2-carboxamide (23c)

To a solution of compound **28a** (100 mg, 0.28 mmol) in MeOH (5 mL), a solution of 1 N HCl/MeOH (0.43 mL, 0.43 mmol) was added. The reaction mixture was stirred for 16 h. Then, a saturated solution of NaHCO₃ was added and the solvent was removed under vacuum. The solid residue was suspended in water and extracted with EtOAc (3 × 10 mL). The organic layer was dried over sodium sulfate, filtered, and concentrated. The crude was purified by column chromatography on silica gel (PE/EtOAc from 3:1 to EtOAc only) to afford the title compound as an amorphous off-white solid (54% yield). ¹H NMR (300 MHz, (CD₃)₂CO) δ 10.47 (s, 1H), 8.75 (s, 1H), 7.48–7.30 (m, 5H), 7.27–7.17 (m, 1H), 7.05 (dd, *J* = 2.6, 1.7 Hz, 1H), 6.87–6.68 (m, 4H), 6.21 (dd, *J* = 3.7, 2.8 Hz, 1H), 4.92 (s, 2H).

N-(Benzyloxy)-1-(3-hydroxyphenyl)-1H-pyrrole-3-carboxamide (23d)

The title compound was prepared according to the procedure used for **23c** starting from **28b** (108 mg, 0.42 mmol) and a solution of 1 N

HCl/MeOH (460 μ L, 0.46 mmol). The crude was purified by column chromatography on silica gel (PE/EtOAc from 4:1 to EtOAc only) to afford the title compound as an amorphous off-white solid (44% yield). ^1H NMR (300 MHz, $(\text{CD}_3)_2\text{CO}$) δ 10.35 (s, 1H), 8.86 (s, 1H), 7.76 (t, $J = 2.0$ Hz, 1H), 7.48 (dd, $J = 7.8, 1.9$ Hz, 2H), 7.42–7.26 (m, 4H), 7.23 (t, $J = 2.6$ Hz, 1H), 7.03 (dd, $J = 8.2, 1.9$ Hz, 2H), 6.86–6.78 (m, 1H), 6.68 (dd, $J = 3.1, 1.7$ Hz, 1H), 4.98 (s, 2H).

Benzyl 1-(3-[[[6-phenylhexyl]carbamoyl]oxy]phenyl)-1H-pyrrole-3-carboxylate (29a)

The title compound was prepared following General Procedure A starting from **23b** (40 mg, 0.14 mmol), TEA (57 μ L, 0.41 mmol), 4-nitrophenyl chloroformate (41 mg, 0.21 mmol), and a solution of the amine **14e** (0.21 mmol, 4.2 mL) in dry DCM. The crude was purified by column chromatography on silica gel (DCM/acetone 100:1) to afford the title compound as a pale-yellow oil (50% yield). ESI-MS m/z : 520 $[\text{M}+\text{Na}]^+$. ^1H NMR (300 MHz, $(\text{CD}_3)_2\text{CO}$) δ 7.95–7.88 (m, 1H), 7.53–7.07 (m, 14H), 6.91 (t, $J = 5.3$ Hz, 1H), 6.73 (dd, $J = 3.0, 1.6$ Hz, 1H), 5.29 (s, 2H), 3.22 (dd, $J = 13.0, 6.8$ Hz, 2H), 2.65–2.56 (m, 2H), 1.70–1.52 (m, 4H), 1.46–1.31 (m, 4H).

3-(3-[[[Benzyl]oxy]carbamoyl]-1H-pyrrol-1-yl]phenyl (6-phenylhexyl) carbamate (29b)

The title compound was prepared following General Procedure A starting from **23d** (20 mg, 0.07 mmol), TEA (29 μ L, 0.21 mmol), 4-nitrophenyl chloroformate (21 mg, 0.10 mmol), and a solution of the amine **14e** (0.10 mmol, 2.1 mL) in dry DCM. The crude was purified by column chromatography on silica gel (DCM/acetone 100:1) to afford the title compound as a pale-yellow oil (24% yield). ^1H NMR (300 MHz, CD_3OD) δ 7.74–7.68 (m, 1H), 7.52–7.04 (m, 15H), 6.66–6.61 (m, 1H), 4.94 (s, 2H), 3.21–3.14 (m, 1H), 3.11–3.04 (m, 1H), 2.60 (dd, $J = 15.6, 8.0$ Hz, 2H), 1.71–1.50 (m, 4H), 1.51–1.30 (m, 4H).

3-(2-[[[Benzyl]oxy]carbamoyl]-1H-pyrrol-1-yl]phenyl (6-phenylhexyl) carbamate (29c)

The title compound was prepared following General Procedure A starting from **23c** (47 mg, 0.15 mmol), TEA (63 μ L, 0.46 mmol), 4-nitrophenyl chloroformate (46 mg, 0.23 mmol), and a solution of the amine **14e** (0.23 mmol, 4.6 mL) in dry DCM. The crude was purified by column chromatography on silica gel (DCM/MeOH 100:1 to 90:1) to afford the title compound as a pale-yellow oil (54% yield). ^1H NMR (300 MHz, $(\text{CD}_3)_2\text{CO}$) δ 10.51 (s, 1H), 7.48–7.06 (m, 15H), 6.94–6.83 (m, 1H), 6.77 (d, $J = 2.2$ Hz, 1H), 6.25–6.19 (m, 1H), 4.93 (s, 2H), 3.20 (dd, $J = 13.1, 6.7$ Hz, 2H), 2.59 (dd, $J = 14.6, 6.7$ Hz, 2H), 1.67–1.52 (m, 4H), 1.47–1.31 (m, 4H).

3-(3-[[[Benzyl]oxy]carbonyl]-1H-pyrrol-1-yl]phenyl 4-(3-phenylpropyl) piperazine-1-carboxylate (30a)

The title compound was prepared following General Procedure A starting from **23b** (28 mg, 0.10 mmol), TEA (40 μ L, 0.29 mmol), 4-nitrophenyl chloroformate (29 mg, 0.14 mmol), and a solution of the amine **14f** (0.14 mmol, 2.9 mL) in dry DCM. The crude was purified by column chromatography on silica gel (Hex/EtOAc 3:1 to 1:1) to afford

the title compound as a pale-yellow oil (50% yield). ESI-MS m/z : 525 $[\text{M}+\text{H}]^+$. ^1H NMR (300 MHz, $(\text{CD}_3)_2\text{CO}$) δ 7.95–7.90 (m, 1H), 7.53–7.11 (m, 15H), 6.73 (dd, $J = 3.0, 1.6$ Hz, 1H), 5.29 (s, 2H), 3.76–3.63 (m, 2H), 3.57–3.46 (m, 2H), 2.67 (dd, $J = 15.5, 7.8$ Hz, 2H), 2.54–2.42 (m, 4H), 2.44–2.28 (m, 2H), 1.88–1.77 (m, 2H).

3-(3-[[[Benzyl]oxy]carbamoyl]-1H-pyrrol-1-yl]phenyl 4-(3-phenylpropyl)piperazine-1-carboxylate (30b)

The title compound was prepared following General Procedure A, starting from **23d** (30 mg, 0.10 mmol), TEA (41 μ L, 0.29 mmol), 4-nitrophenyl chloroformate (29 mg, 0.15 mmol), and a solution of the amine **14f** (0.15 mmol, 2.9 mL) in dry DCM. The crude was purified by column chromatography on Al_2O_3 (PE/EtOAc 2:1 to EtOAc/MeOH 100:1) to afford the title compound as a pale-yellow oil (80% yield). ^1H NMR (300 MHz, CD_3OD) δ 7.74–7.71 (m, 1H), 7.52–7.44 (m, 3H), 7.43–7.31 (m, 5H), 7.29–7.06 (m, 7H), 6.64 (s, 1H), 4.94 (s, 2H), 3.78–3.68 (m, 2H), 3.61–3.52 (m, 2H), 2.71–2.60 (m, 2H), 2.59–2.50 (m, 3H), 2.50–2.40 (m, 3H), 1.95–1.78 (m, 2H).

3-(3-Carbamoyl-1H-pyrrol-1-yl)phenyl (6-[4-[[[benzyl]oxy]carbamoyl]phenyl]hexyl)carbamate (31a)

The title compound was prepared following General Procedure A, starting from **23e** (25 mg, 0.13 mmol), TEA (52 μ L, 0.38 mmol), 4-nitrophenyl chloroformate (38 mg, 0.19 mmol), and a solution of the amine **14b** (0.19 mmol, 3.8 mL) in dry DCM. The crude was purified by column chromatography on silica gel (DCM/MeOH/ NH_4OH 30:1) to afford the title compound as a white solid (27% yield). ESI-MS m/z : 577 $[\text{M}+\text{H}]^+$. ^1H NMR (300 MHz, CDCl_3) δ 7.74–7.68 (m, 1H), 7.63–7.56 (m, 2H), 7.48–7.34 (m, 6H), 7.26 (d, $J = 1.3$ Hz, 2H), 7.25–7.16 (m, 3H), 7.11–7.04 (m, 1H), 7.03–6.99 (m, 1H), 5.03 (s, 2H), 3.24 (dd, $J = 13.1, 6.6$ Hz, 2H), 2.64 (t, $J = 7.5$ Hz, 2H), 1.70–1.51 (m, 4H), 1.44–1.29 (m, 4H).

3-(3-Carbamoyl-1H-pyrrol-1-yl)phenyl 4-[3-(4-[[[tetrahydro-2H-pyran-2-yl]oxy]carbamoyl]phenyl)propyl]piperazine-1-carboxylate (31b)

The title compound was prepared following General Procedure A, starting from **23e** (17 mg, 0.08 mmol), TEA (35 μ L, 0.25 mmol), 4-nitrophenyl chloroformate (25 mg, 0.13 mmol), and a solution of the amine **14c** (0.10 mmol, 2.6 mL) in dry DCM. The crude was purified by column chromatography on silica gel (EtOAc to EtOAc/MeOH 3:1) to afford the title compound as a light brown solid (37% yield). ESI-MS m/z : 575.2 $[\text{M}+\text{H}]^+$, 598.2 $[\text{M}+\text{Na}]^+$. ^1H NMR (300 MHz, CD_3OD) δ 7.80 (t, $J = 2.0$ Hz, 1H), 7.71 (d, $J = 8.2$ Hz, 2H), 7.48 (t, $J = 8.1$ Hz, 1H), 7.43–7.35 (m, 1H), 7.35–7.23 (m, 2H), 7.22 (t, $J = 2.7$ Hz, 1H), 7.12–7.02 (m, 1H), 6.78–6.66 (m, 1H), 5.08–5.00 (m, 1H), 4.20–4.05 (m, 1H), 3.76–3.49 (m, 5H), 2.72 (t, $J = 7.5$ Hz, 2H), 2.59–2.48 (m, 4H), 2.48–2.36 (m, 2H), 1.97–1.73 (m, 6H), 1.73–1.53 (m, 3H).

3-(3-Carbamoyl-1H-pyrrol-1-yl)phenyl 4-(4-[[[tetrahydro-2H-pyran-2-yl]oxy]carbamoyl]benzyl)piperazine-1-carboxylate (31c)

The title compound was prepared following General Procedure A, starting from **23e** (34 mg, 0.17 mmol), TEA (70 μ L, 0.50 mmol),

4-nitrophenyl chloroformate (50 mg, 0.25 mmol), and a solution of the amine **14d** (0.20 mmol, 5.0 mL) in dry DCM. The crude was purified by column chromatography on silica gel (EtOAc to EtOAc/MeOH 3:1) to afford the title compound as a light brown solid (50% yield). ESI-MS m/z : 570.2 [M+Na]⁺; 464.1 [M-THP]⁺. ¹H NMR (300 MHz, CD₃OD) δ 7.79–7.71 (m, 3H), 7.59–7.40 (m, 4H), 7.43–7.27 (m, 1H), 7.22–7.19 (m, 1H), 7.10–7.01 (m, 1H), 6.77–6.68 (m, 1H), 5.05 (t, J = 2.8 Hz, 1H), 4.19–4.05 (m, 1H), 3.77–3.47 (m, 7H), 2.49 (t, J = 5.0 Hz, 4H), 1.96–1.75 (m, 3H), 1.71–1.56 (m, 3H).

Methyl 1-(3-[[[6-phenylhexyl]carbamoyl]oxy]phenyl)-1H-pyrrole-3-carboxylate (4a)

The title compound was prepared following General Procedure A, starting from **23a** (37 mg, 0.17 mmol), TEA (71 μ L, 0.51 mmol), 4-nitrophenyl chloroformate (52 mg, 0.26 mmol), and a solution of the amine **14e** (0.26 mmol, 5.2 mL) in dry DCM. The crude was purified by column chromatography on silica gel (PE/EtOAc 1:1) to afford the title compound as a pale-yellow oil (34% yield). ¹H NMR (300 MHz, CDCl₃) δ 7.70–7.65 (m, 1H), 7.42 (t, J = 8.3 Hz, 1H), 7.33–7.13 (m, 7H), 7.11–7.05 (m, 1H), 7.00 (t, J = 2.6 Hz, 1H), 6.74 (dd, J = 3.0, 1.6 Hz, 1H), 5.04 (t, J = 6.4, 5.6 Hz, 1H), 3.84 (s, 3H), 3.26 (dd, J = 13.4, 6.7 Hz, 2H), 2.66–2.57 (m, 2H), 1.72–1.53 (m, 4H), 1.45–1.33 (m, 4H). ¹³C NMR (75 MHz, CDCl₃) δ 165.0, 154.0, 151.9, 142.6, 140.6, 130.3, 128.4, 128.3, 125.7, 124.4, 120.6, 120.0, 118.0, 117.5, 114.6, 111.7, 51.3, 41.3, 35.9, 31.4, 29.7, 28.9, 26.6. HRMS(ESI) m/z [M+H]⁺ calcd for [C₂₅H₂₉N₂O₄]⁺ 421.2122, found 421.2107; m/z [M+Na]⁺ calcd for [C₂₅H₂₈N₂O₄Na]⁺ 443.1941, found 443.1925; m/z [M+K]⁺ calcd for [C₂₅H₂₈N₂O₄K]⁺ 459.1681; found 459.1659.

1-(3-[[[6-Phenylhexyl]carbamoyl]oxy]phenyl)-1H-pyrrole-3-carboxylic acid (4b)

The title compound was prepared following General Procedure B, starting from **29a** (50 mg, 0.10 mmol) and Pd/C 10% (0.01 mol). The crude was purified by column chromatography on silica gel (DCM/MeOH 20:1 to DCM/MeOH/HCOOH 20:1:0.1) to afford the title compound as a pale-yellow oil (69% yield). ESI-MS m/z : 407 [M+Na]⁺. ¹H NMR (300 MHz, CD₃OD) δ 7.82–7.77 (m, 1H), 7.47 (t, J = 8.1 Hz, 1H), 7.41–7.34 (m, 1H), 7.31 (t, J = 2.0 Hz, 1H), 7.27–7.04 (m, 7H), 6.69 (dd, J = 3.0, 1.6 Hz, 1H), 3.17 (t, J = 7.0 Hz, 2H), 2.63–2.57 (m, 2H), 1.69–1.47 (m, 4H), 1.47–1.32 (m, 4H). ¹³C NMR (75 MHz, CD₃OD) δ 167.1, 155.3, 152.2, 142.5, 140.5, 130.1, 127.98, 127.8, 125.2, 124.3, 120.5, 119.7, 118.3, 116.8, 114.0, 111.4, 40.6, 35.4, 31.3, 29.2, 28.6, 26.3. HRMS(ESI) m/z [M+Na]⁺ calcd for [C₂₄H₂₆N₂O₄Na]⁺ 429.1785, found 429.1765.

3-[3-(Hydroxycarbamoyl)-1H-pyrrol-1-yl]phenyl (6-phenylhexyl) carbamate (4c)

The title compound was prepared following General Procedure B, starting from **29b** (34 mg, 0.07 mmol) and Pd/C 10% (0.007 mmol) in EtOAc/MeOH 3:1 (4 mL). The crude was purified by column chromatography on silica gel (DCM/MeOH 30:1 to DCM/MeOH/HCOOH 10:1:0.1) to afford the title compound as an amorphous brown solid (58% yield). ¹H NMR (300 MHz, CD₃OD) δ 7.81–7.64 (m,

1H), 7.52–7.01 (m, 10H), 6.65 (s, 1H), 3.23–3.09 (m, 2H), 2.61 (t, J = 7.5 Hz, 2H), 1.77–1.49 (m, 4H), 1.46–1.19 (m, 4H). ¹³C NMR (75 MHz, CD₃OD) δ 164.2, 155.3, 152.3, 142.4, 140.5, 130.1, 128.0, 127.8, 125.2, 121.2, 120.3, 119.5, 118.3, 116.7, 113.9, 109.0, 40.6, 35.4, 31.3, 29.2, 28.6, 26.3. HRMS(ESI) m/z [M+Na]⁺ calcd for [C₂₄H₂₇N₃O₄Na]⁺ 444.1894, found 444.1882.

3-[2-(Hydroxycarbamoyl)-1H-pyrrol-1-yl]phenyl (6-phenylhexyl) carbamate (4d)

The title compound was prepared following General Procedure B, starting from **29c** (41 mg, 0.08 mmol) and Pd/C 10% (0.008 mmol) in EtOAc/MeOH 3:1 (4 mL). The crude was purified by column chromatography on silica gel EtOAc/PE 2:1 to EtOAc only) to afford the title compound as an amorphous brown solid (12% yield). ¹H NMR (300 MHz, CD₃OD) δ 7.44–7.35 (m, 1H), 7.27–7.05 (m, 9H), 6.72 (dd, J = 3.7, 1.6 Hz, 1H), 6.28–6.23 (m, 1H), 3.16 (t, J = 6.9 Hz, 2H), 2.61 (t, J = 7.7 Hz, 2H), 1.70–1.48 (m, 4H), 1.46–1.31 (m, 4H). ¹³C NMR (75 MHz, CD₃OD) 168.3, 155.3, 152.3, 142.5, 140.6, 130.1, 127.9, 127.8, 125.2, 122.0, 120.7, 120.3, 119.6, 116.7, 113.9, 109.9, 40.6, 35.4, 31.2, 29.2, 28.5, 26.3. HRMS(ESI) m/z [M+H]⁺ calcd for [C₂₄H₂₈N₃O₄]⁺ 422.2074, found 422.2058; m/z [M+Na]⁺ calcd for [C₂₄H₂₇N₃O₄Na]⁺ 444.1894, found 444.1878 m/z [M+K]⁺ calcd for [C₂₄H₂₇N₃O₄K]⁺ 460.1633, found 460.1615.

1-(3-[[4-(3-Phenylpropyl)piperazine-1-carbonyl]oxy]phenyl)-1H-pyrrole-3-carboxylic acid (4e)

The title compound was prepared following General Procedure B, starting from **30a** (21 mg, 0.04 mmol) and Pd/C 10% (0.004 mmol) in EtOAc/MeOH 3:1 (4 mL). The crude was purified by column chromatography on silica gel (DCM/MeOH 20:1 to DCM/MeOH/HCOOH 20:1:0.1) to afford the title compound as a pale-yellow oil (40% yield). ESI-MS m/z : 434 [M+H]⁺. ¹H NMR (300 MHz, CD₃OD) δ 7.87–7.73 (m, 1H), 7.51–7.31 (m, 3H), 7.29–7.06 (m, 7H), 6.69 (dd, J = 3.0, 1.6 Hz, 1H), 3.78–3.57 (m, 4H), 2.71–2.54 (m, 6H), 2.53–2.44 (m, 2H), 1.95–1.81 (m, 2H). ¹³C NMR (75 MHz, CD₃OD) 167.5, 153.5, 152.2, 141.7, 140.6, 130.2, 128.0, 128.0, 125.5, 124.1, 120.3, 119.7, 118.9, 117.1, 114.1, 111.5, 57.4, 52.3, 43.2, 33.0, 27.8. HRMS(ESI) m/z [M+H]⁺ calcd for [C₂₅H₂₈N₃O₄]⁺ 434.2074, found 434.2061.

3-[3-(Hydroxycarbamoyl)-1H-pyrrol-1-yl]phenyl 4-(3-phenylpropyl) piperazine-1-carboxylate (4f)

The title compound was prepared following General Procedure B, starting from **30b** (42 mg, 0.08 mmol) and Pd/C 10% (0.008 mmol) in EtOAc/MeOH 3:1 (4 mL). The crude was purified by column chromatography on silica gel (DCM/MeOH 40:1 to DCM/MeOH/NH₄OH 10:1:0.1) to afford the title compound as an amorphous brown solid (61% yield). ¹H NMR (300 MHz, CD₃OD) δ 7.73 (s, 1H), 7.55–7.00 (m, 10H), 6.65 (s, 1H), 3.75–3.48 (m, 4H), 2.73–2.40 (m, 8H), 1.96–1.76 (m, 2H). ¹³C NMR (75 MHz, CD₃OD) δ 164.2, 153.3, 152.2, 141.4, 140.6, 130.2, 128.0 (2C), 125.6, 121.2, 120.3, 119.6, 118.4, 117.1, 114.0, 109.0, 57.2, 52.2, 43.4, 42.9, 32.9, 29.3, 27.5. HRMS(ESI) m/z [M+H]⁺ calcd for [C₂₅H₂₉N₄O₄]⁺ 449.2183, found 449.2170.

Methyl 4-(6-(((3-(3-carbamoyl-1H-pyrrol-1-yl)phenoxy)carbonyl)amino)hexyl)benzoate (4g)

The title compound was prepared following General Procedure A, starting from **23e** (17 mg, 0.08 mmol), TEA (35 μ L, 0.25 mmol), 4-nitrophenyl chloroformate (25 mg, 0.13 mmol), and a solution of the amine **14a** (0.13 mmol, 2 mL) in dry DCM. The crude was purified by column chromatography on silica gel (DCM/MeOH 50:1 to 40:1) to afford the title compound as an amorphous white solid (54% yield). ^1H NMR (300 MHz, CDCl_3) δ 7.94 (d, $J = 8.3$ Hz, 2H), 7.66 (t, $J = 2.0$ Hz, 1H), 7.40 (t, $J = 8.0$ Hz, 1H), 7.30–7.14 (m, 5H), 7.12–7.03 (m, 1H), 7.04–6.96 (m, 1H), 6.57 (dd, $J = 3.0, 1.7$ Hz, 1H), 5.21 (t, $J = 5.7$ Hz, 1H), 3.32–3.19 (m, 2H), 2.71–2.60 (m, 2H), 1.83–1.46 (m, 4H), 1.44–1.32 (m, 4H). ^{13}C NMR (75 MHz, CDCl_3) δ 163.3, 163.0, 150.2, 148.0, 144.2, 136.4, 126.5, 125.7, 124.5, 123.7, 119.3, 116.9, 116.1, 115.7, 113.5, 110.6, 105.9, 48.1, 37.3, 31.9, 27.0, 25.7, 24.9, 22.6. HRMS(ESI) m/z $[\text{M}+\text{H}]^+$ calcd for $[\text{C}_{26}\text{H}_{30}\text{N}_5\text{O}_5]^+$ 464.2180, found 464.2166; m/z $[\text{M}+\text{Na}]^+$ calcd for $[\text{C}_{26}\text{H}_{29}\text{N}_5\text{O}_5\text{Na}]^+$ 486.1999, found 486.1976; m/z $[\text{M}+\text{K}]^+$ calcd for $[\text{C}_{26}\text{H}_{29}\text{N}_5\text{O}_5\text{K}]^+$ 502.1739, found 502.1723.

3-(3-Carbamoyl-1H-pyrrol-1-yl)phenyl {6-[4-(hydroxycarbamoyl)phenyl]hexyl}carbamate (4h)

The title compound was prepared following General Procedure B, starting from **31a** (19 mg, 0.03 mmol) and Pd/C 10% (0.003 mmol) in EtOAc/MeOH 1:2 (2.1 mL). The crude was purified by column chromatography on silica gel (DCM/MeOH 20:1 to DCM/MeOH/NH₄OH 10:1:0.1) to afford the title compound as an amorphous light brown solid (39% yield). ESI-MS m/z : 465.6 $[\text{M}+\text{H}]^+$. ^1H NMR (300 MHz, DMSO- d_6) 11.10 (s, 1H), 8.94 (s, 1H), 7.90 (s, $J = 27.4$ Hz, 1H), 7.81 (t, $J = 5.2$ Hz, 1H), 7.64 (d, $J = 8.0$ Hz, 2H), 7.52–7.32 (m, 4H), 7.25 (d, $J = 7.9$ Hz, 2H), 7.00 (d, $J = 6.4$ Hz, 1H), 6.87 (s, 1H), 6.63 (s, 1H), 3.15 (d, $J = 5.2$ Hz, 1H), 3.09–2.97 (m, 2H), 2.60 (t, $J = 7.6$ Hz, 2H), 1.66–1.40 (m, 4H), 1.39–1.25 (m, 4H). ^{13}C NMR (75 MHz, DMSO- d_6) 165.5, 164.7, 154.4, 152.5, 146.2, 140.5, 130.8, 130.7, 128.7, 127.3, 122.7, 121.8, 120.4, 119.8, 116.4, 113.7, 110.9, 35.3, 31.1, 29.5, 29.4, 28.8, 26.5. HRMS(ESI) m/z $[\text{M}+\text{H}]^+$ calcd for $[\text{C}_{25}\text{H}_{29}\text{N}_4\text{O}_5]^+$ 465.2132, found 465.2116; m/z $[\text{M}+\text{Na}]^+$ calcd for $[\text{C}_{25}\text{H}_{28}\text{N}_4\text{O}_5\text{Na}]^+$ 487.1952, found 487.1928; m/z $[\text{M}+\text{K}]^+$ calcd for $[\text{C}_{25}\text{H}_{28}\text{N}_4\text{O}_5\text{K}]^+$ 503.1691, found 503.1673.

3-(3-Carbamoyl-1H-pyrrol-1-yl)phenyl 4-{3-[4-(hydroxycarbamoyl)phenyl]propyl}piperazine-1-carboxylate (4i)

The title compound was prepared following General Procedure C, starting from compound **31b**. The crude was purified by column chromatography on silica gel ($\text{CHCl}_3/\text{MeOH}/\text{NH}_4\text{OH}$ 20:1:0.1 to 5:1:0.1) to afford the title compound as an amorphous light brown solid (53% yield). ESI-MS m/z : 492.2 $[\text{M}+\text{H}]^+$; 514.2 $[\text{M}+\text{Na}]^+$. ^1H NMR (300 MHz, CD_3OD) δ 7.80 (t, $J = 2.0$ Hz, 1H), 7.72–7.63 (m, 2H), 7.48 (t, $J = 8.1$ Hz, 1H), 7.47–7.36 (m, 1H), 7.36–7.28 (m, 3H), 7.23 (t, $J = 2.7$ Hz, 1H), 7.13–7.03 (m, 1H), 6.72 (dd, $J = 3.1, 1.6$ Hz, 1H), 3.75–3.42 (m, 4H), 2.72 (t, $J = 7.5$ Hz, 2H), 2.56–2.50 (m, 4H), 2.49–2.38 (m, 2H), 1.97–1.80 (m, 2H). ^{13}C NMR (75 MHz, CD_3OD) δ 168.2, 166.7, 153.5, 151.5, 146.1, 140.7, 130.2, 129.8, 128.4, 126.8,

122.1, 120.8, 120.3, 119.6, 117.0, 114.0, 110.0, 57.2, 52.3, 43.9, 43.3, 32.9, 29.3, 27.5. HRMS(ESI) m/z $[\text{M}+\text{H}]^+$ calcd for $[\text{C}_{26}\text{H}_{30}\text{N}_5\text{O}_5]^+$ 492.2242, found 492.2219; m/z $[\text{M}+\text{Na}]^+$ calcd for $[\text{C}_{26}\text{H}_{29}\text{N}_5\text{O}_5\text{Na}]^+$ 514.2061, found 514.2042.

3-(3-Carbamoyl-1H-pyrrol-1-yl)phenyl 4-[4-(hydroxycarbamoyl)benzyl]piperazine-1-carboxylate (4j)

The title compound was prepared following General Procedure C, starting from compound **31c**. The crude was purified by column chromatography on silica gel ($\text{CHCl}_3/\text{MeOH}/\text{NH}_4\text{OH}$ 20:1:0.1–5:1:0.1) to afford the title compound as an amorphous light brown solid (80% yield). ESI-MS m/z : 464.1 $[\text{M}+\text{H}]^+$; 486.1 $[\text{M}+\text{Na}]^+$. ^1H NMR (300 MHz, CD_3OD) δ 7.80 (s, 1H), 7.73 (d, $J = 8.1$ Hz, 2H), 7.53–7.42 (m, 3H), 7.41–7.34 (m, 1H), 7.37–7.29 (m, 1H), 7.22 (t, $J = 2.6$ Hz, 1H), 7.12–7.03 (m, 1H), 6.72 (dd, $J = 3.2, 1.5$ Hz, 1H), 3.78–3.67 (m, 2H), 3.63 (s, 2H), 3.60–3.52 (m, 2H), 2.59–2.47 (m, 4H). ^{13}C NMR (75 MHz, CD_3OD) δ 168.2, 166.5, 153.5, 152.3, 141.5, 140.7, 131.2, 130.2, 129.1, 126.8, 122.1, 120.8, 120.3, 119.6, 117.0, 114.0, 110.0, 61.8, 52.3, 44.2, 43.2, 29.3. HRMS(ESI) m/z $[\text{M}+\text{H}]^+$ calcd for $[\text{C}_{24}\text{H}_{26}\text{N}_5\text{O}_5]^+$ 464.1928, found 464.1908; m/z $[\text{M}+\text{Na}]^+$ calcd for $[\text{C}_{24}\text{H}_{25}\text{N}_5\text{O}_5\text{Na}]^+$ 486.1748, found 486.1725; m/z $[\text{M}+\text{K}]^+$ calcd for $[\text{C}_{24}\text{H}_{25}\text{N}_5\text{O}_5\text{K}]^+$ 502.1487, found 502.1464.

4.2 | ESI-HRMS, purity, solubility, and chemical stability analysis

4.2.1 | ESI-HRMS

For the ESI-HRMS analysis each compound, previously purified by chromatographic methods, was dissolved in methanol (MeOH hypergrade for LC-MS, LiChrosolv[®], Merck Sigma-Aldrich), and infused directly into the ion source of the mass spectrometer at a flow rate of 20 $\mu\text{L}/\text{min}$.

4.2.2 | HPLC analysis

For the HPLC analysis a Chromolith HPLC column RP-18 was employed. The runs were performed by a gradient elution starting from a mixture of 10% MeCN (0.1% TFA as phase modifier) in H₂O (0.1% TFA as phase modifier) to 90% MeCN (0.1% TFA) in H₂O (0.1% TFA) in 20 min, followed by 3 min of isocratic elution at 90% MeCN (0.1% TFA) in H₂O (0.1% TFA) and 3 min of reconditioning. The flow speed was settled at 1.0 mL/min and the temperature was maintained at 25°C. The volume of injection of the sample was 10 μL and the wavelength selected for the detection was 254 nm.

4.2.3 | Solubility and chemical stability at 25°C

Solubility and chemical stability values, both calculated at pH = 3.0 and pH = 7.4 after 24 h, were obtained by applying our previously

described procedures.^[16] For each sample, the analysis was performed in triplicate.

4.3 | Enzymatic assays

4.3.1 | Enzymatic assays on *human* HDACs

For the evaluation of their inhibitory activity, different concentrations of the novel compounds were incubated in a low-binding black 96-well plate with 30 ng of *human* recombinant HDAC6 (BPS Bioscience; Cat. # 50056), *human* recombinant HDAC1 (BPS Bioscience; Cat. # 50051), *human* recombinant HDAC8 (BPS Bioscience; Cat. # 50008), or 500 ng of *human* recombinant HDAC10 (BPS Bioscience; Cat. # 50060) in an assay buffer composed of 25 mM Tris/HCl, pH 8.0, 137 mM NaCl, 2.7 mM KCl, 1 mM MgCl₂, and 0.1 mg/mL bovine serum albumin for 30 min at 37°C. At the end of the incubation, the deacetylation reaction was initiated by adding 200 μM of the fluorogenic acetylated HDAC substrate 3 (BPS Bioscience; Cat. # 50037) for HDAC6, HDAC1, and HDAC10 assays, or of the fluorogenic HDAC substrate class 2A (BPS Bioscience; Cat. # 50040) for HDAC8 assays. After 30 min at 37°C, the reaction was stopped by the addition of an HDAC assay developer (BPS Bioscience; Cat. # 50060). Following an incubation of 15 min at room temperature, fluorescence was measured in an EnSight multimodal plate reader (PerkinElmer) with an excitation wavelength of 360 nm and an emission wavelength of 450 nm.

4.3.2 | Enzymatic assays on *human* FAAH

The inhibition activity of the novel compounds against *human* FAAH was assessed using a fluorescence-based assay, following the manufacturer's instructions (Cayman Chemical). Briefly, the compounds were preincubated at various concentrations with human FAAH for 30 min at 37°C. The reaction was initiated by adding 7-amino-4-methylcoumarin (AMC) arachidonoyl amide (final concentration 1 μM) as the substrate. After a 30-min incubation at 37°C, the fluorescence resulting from the release of the AMC product was measured using an excitation wavelength of 355 nm and an emission wavelength of 465 nm, utilizing an EnSight Multimode plate reader (Perkin Elmer).

4.3.3 | Enzymatic assays on *human* MAGL

The inhibitory activity of the novel compounds against *human* MAGL was evaluated using a fluorescence-based assay, following the manufacturer's instructions (Biovision). Briefly, the compounds were preincubated at various concentrations with human MAGL for 30 min at 37°C. After adding the substrate, the assay mixture was further incubated for 30 min at 37°C, and the resulting fluorescence was measured using an excitation wavelength of 360 nm and an emission wavelength of 460 nm, employing an EnSight Multimode plate reader (Perkin Elmer).

4.4 | Molecular docking

Molecular docking studies were conducted employing Glide software (Glide, Schrödinger, LLC, release 2016) via Maestro Drug Discovery suite release 2015.^[53,54] The X-ray crystal structures of FAAH covalently bound to an alpha-ketoheterocycle inhibitor (PDB code: 3K84, chain A) and human HDAC6 CD2 domain in complex with trichostatin A (PDB code: 5EDU, chain A) were downloaded from RCSB Protein Data Bank and treated with Protein Preparation Wizard (PPW)^[55] (PPW, Schrödinger, LLC, 2016) protocol implemented in Maestro suite for obtaining appropriate protein structures. Concerning the FAAH enzyme, the protein was refined setting the pH value at 9.0, at which the enzyme shows its maximum activity^[56]; the catalytic Lys142 was modeled in its neutral form, in accordance with the catalytic mechanism of FAAH.^[57] Ligands were built in the Maestro suite using available drawing tools. Compounds were minimized using MacroModel software (MacroModel, Schrödinger, LLC, 2016) with OPLS-2005 as a force field and the generalized-born/surface-area (GB/SA) model to simulate the solvent effects. No cut-off for nonbonded interactions was used. PRCG method was employed with 2500 maximum iterations and 0.001 gradient convergence threshold for performing the molecular energy minimizations. MCMM was employed as a torsional sampling method for the conformational searches, performing automatic setup with 21 kJ/mol (5.02 kcal/mol) in the energy window for saving structure and 0.5 Å was used as a cut-off distance for redundant conformers. The resulting molecules were submitted to the LigPrep application (LigPrep, Schrödinger, LLC, release 2016) for generating the most probable ionization state at suitable pH values (7.4 ± 0.2 for HDAC6, 9.0 ± 0.2 for FAAH). Energy grids were prepared using Glide for both the enzymes using default value of protein atom scaling factor (1.0 Å) within cubic boxes centered on the center of mass of the respective co-crystallized ligand. In the case of HDAC6, metal constraints were introduced in the Zn²⁺ ion, while for FAAH H-bond constraints between the oxyanion hole nitrogen of Ile238 and Gly239 and the carbonylic oxygen atom of **4a-j** were added. Docking studies were performed using the extra precision (XP) mode and were forced to satisfy the previously defined constraints. The number of poses entered for post-docking minimization was set to 50. MM/GBSA calculations were performed on the docking poses using Prime (Prime, Schrödinger, LLC, 2016) tool with OPLS2005 force field and VSGB solvation model.^[56,58,59]

4.5 | Cellular studies

4.5.1 | Cell culture

1321N1 astrocyte cell line (Sigma-Aldrich) was maintained in DMEM (Invitrogen) supplemented with 10% FBS (Thermo Scientific), L-glutamine (2 mM), penicillin (100 U/mL) and streptomycin (100 μg/mL) in a humidified atmosphere (5% CO₂) at 37°C. SH-SY5Y were purchased from American Type Culture Collection) and maintained in a 1:1 mixture

of Eagle's minimum essential medium and F12 medium supplemented with 10% FBS, penicillin (100 U/mL), and streptomycin (100 µg/mL) at 37°C in a humidified atmosphere with 5% CO₂.

4.5.2 | ROS production assay

ROS production was evaluated through the Total Reactive Oxygen Species Assay Kit (Thermo-Fisher, cat. n. 88-5930-74). 1321N1 or SH-SY5Y were seeded into 96-well microculture plates at a density of 1×10^4 cells/well and incubated overnight in a humidified atmosphere (5% CO₂) at 37°C. Afterward, the cells were treated for 24 h with the novel selected compounds or NAC. Subsequently, 10 µl of ROS Assay Stain was added directly to the culture media, and the cells were incubated for 60 min at 37°C. The cells were then exposed to 50 µM TBHP to induce the production of ROS. After a 1-h incubation at 37°C, fluorescence was measured with an excitation wavelength of 488 nm and an emission wavelength of 520 nm, employing an EnSight Multimode plate reader (Perkin Elmer).

4.5.3 | Cell viability assay

1321N1 or SH-SY5Y cell viability was assessed using a 3-(4,5-dimethyl-2-thiazolyl)-2,5-diphenyl-2H-tetrazolium bromide (MTT) assay. The cells were harvested from culture flasks through trypsinization and then seeded into 96-well microculture plates at a density of 1×10^4 cells/well. Subsequently, they were incubated overnight in a humidified atmosphere (5% CO₂) at 37°C. After the incubation with the novel compounds, TBHP or glutamate, 15 µL of a 5 mg/ml MTT solution in PBS was added to each well, followed by a 4-h incubation in the dark. During this time, MTT is transformed into formazan by mitochondrial dehydrogenase in viable cells. After the incubation, formazan crystals were solubilized by adding 150 µL of an acidified isopropanol solution. Optical densities at 570 nm were measured using the EnSight multimode plate reader (Perkin Elmer).

4.5.4 | Data and statistical analysis

IC₅₀ data are expressed as mean ± SEM of three independent experiments performed in triplicate. All statistical analyses were performed with GraphPad Prism 8.0.1. The differences between groups were analyzed using one-way analysis of variance followed by Tukey's multiple comparisons test.

ACKNOWLEDGMENTS

The authors wish to thank MIUR-PRIN n° 20175SA5JJ for financial support. K. V. thank the Ministry of University and Research (MUR) National Recovery and Resilience Plan (NRRP), Project no. PE00000006 CUP H93C22000660006—MNESYS, a multiscale integrated approach to the study of the nervous system in health and disease (DN. 1553 11.10.2022).

CONFLICT OF INTEREST STATEMENT

The authors declare no conflict of interest.

ORCID

Ilaria Corsaro  <https://orcid.org/0000-0001-7034-3162>

Silvia Pasquini  <http://orcid.org/0000-0001-9442-1428>

Stefania Butini  <http://orcid.org/0000-0002-8471-0880>

REFERENCES

- [1] A. Anighoro, J. Bajorath, G. Rastelli, *J. Med. Chem.* **2014**, *57*, 7874.
- [2] A. Papa, S. Pasquini, C. Contri, S. Gemma, G. Campiani, S. Butini, K. Varani, F. Vincenzi, *Cells* **2022**, *11*, 471. <https://doi.org/10.3390/cells11030471>
- [3] F. Aiello, G. Carullo, M. Badolato, A. Brizzi, *ChemMedChem* **2016**, *11*, 1686.
- [4] M. L. Bolognesi, A. Cavalli, *ChemMedChem* **2016**, *11*, 1190.
- [5] R. Morphy, Z. Rankovic, *J. Med. Chem.* **2005**, *48*, 6523.
- [6] K. V. Butler, J. Kalin, C. Brochier, G. Vistoli, B. Langley, A. P. Kozikowski, *J. Am. Chem. Soc.* **2010**, *132*, 10842.
- [7] P. E. Castillo, T. J. Younts, A. E. Chávez, Y. Hashimoto-dani, *Neuron* **2012**, *76*, 70.
- [8] H.-C. Lu, K. Mackie, *Biol. Psychiatry* **2016**, *79*, 516.
- [9] F. De Fonseca, I. Del Arco, F. J. Bermudez-Silva, A. Bilbao, A. Cippitelli, M. Navarro, *Alcohol and Alcoholism* **2005**, *40*, 2.
- [10] A. Kreitzer, *Curr. Opin. Neurobiol.* **2002**, *12*, 324.
- [11] B. S. Basavarajappa, M. Shivakumar, V. Joshi, S. Subbanna, *J. Neurochem.* **2017**, *142*, 624.
- [12] A. Duranti, G. Beldarrain, A. Álvarez, M. Sbriscia, S. Carloni, W. Balduini, D. Alonso-Alconada, *Biomedicines* **2022**, *11*, 28.
- [13] A. J. Sánchez, A. García-Merino, *Clin. Immunol.* **2012**, *142*, 57.
- [14] S. Butini, M. Brindisi, S. Gemma, P. Minetti, W. Cabri, G. Gallo, S. Vincenti, E. Talamonti, F. Borsini, A. Caprioli, M. A. Stasi, S. Di Serio, S. Ros, G. Borrelli, S. Maramai, F. Fezza, G. Campiani, M. Maccarrone, *J. Med. Chem.* **2012**, *55*, 6898.
- [15] M. Brindisi, G. Borrelli, S. Brogi, A. Grillo, S. Maramai, M. Paolino, M. Benedusi, A. Pecorelli, G. Valacchi, L. Di Cesare Mannelli, C. Ghelardini, M. Allarà, A. Ligresti, P. Minetti, G. Campiani, V. Di Marzo, S. Butini, S. Gemma, *ChemMedChem* **2018**, *13*, 2090.
- [16] A. Grillo, G. Chemi, S. Brogi, M. Brindisi, N. Relitti, F. Fezza, D. Fazio, L. Castelletti, E. Perdona, A. Wong, S. Lamponi, A. Pecorelli, M. Benedusi, M. Fantacci, M. Valoti, G. Valacchi, F. Micheli, E. Novellino, G. Campiani, S. Butini, M. Maccarrone, S. Gemma, *Eur. J. Med. Chem.* **2019**, *183*, 111674.
- [17] A. Papa, S. Pasquini, F. Galvani, M. Cammarota, C. Contri, G. Carullo, S. Gemma, A. Ramunno, S. Lamponi, B. Gorelli, S. Saponara, K. Varani, M. Mor, G. Campiani, F. Boscia, F. Vincenzi, A. Lodola, S. Butini, *Eur. J. Med. Chem.* **2023**, *246*, 114952.
- [18] T. C. S. Ho, A. H. Y. Chan, A. Ganesan, *J. Med. Chem.* **2020**, *63*, 12460.
- [19] G. Li, Y. Tian, W.-G. Zhu, *Front. Cell. Dev. Biol.* **2020**, *8*, 576946.
- [20] J. Tang, H. Yan, S. Zhuang, *Clin. Sci.* **2013**, *124*, 651.
- [21] G. Campiani, C. Cavella, J. D. Osko, M. Brindisi, N. Relitti, S. Brogi, A. P. Saraswati, S. Federico, G. Chemi, S. Maramai, G. Carullo, B. Jaeger, A. Carleo, R. Benedetti, F. Sarno, S. Lamponi, P. Rottoli, E. Bargagli, C. Bertucci, D. Tedesco, D. Herp, J. Senger, G. Ruberti, F. Saccoccia, S. Saponara, B. Gorelli, M. Valoti, B. Kennedy, H. Sundaramurthi, S. Butini, M. Jung, K. M. Roach, L. Altucci, P. Bradding, D. W. Christianson, S. Gemma, A. Prasse, *J. Med. Chem.* **2021**, *64*, 9960.
- [22] R. Adalbert, A. Kaieda, C. Antoniou, A. Loreto, X. Yang, J. Gilley, T. Hoshino, K. Uga, M. T. Makhija, M. P. Coleman, *ACS Chem. Neurosci.* **2020**, *11*, 258.
- [23] P. LoPresti, *Cells* **2020**, *10*, 12.

- [24] D.-M. Chuang, Y. Leng, Z. Marinova, H.-J. Kim, C.-T. Chiu, *Trends Neurosci.* **2009**, *32*, 591.
- [25] H. Maruoka, H. Sasaya, K. Sugihara, K. Shimoke, T. Ikeuchi, *J. Biochem.* **2011**, *150*, 473.
- [26] G. Carullo, S. Federico, N. Relitti, S. Gemma, S. Butini, G. Campiani, *ACS Chem. Neurosci.* **2020**, *11*, 2173.
- [27] M. Brindisi, A. P. Saraswati, S. Brogi, S. Gemma, S. Butini, G. Campiani, *J. Med. Chem.* **2020**, *63*, 23.
- [28] F. Yang, N. Zhao, D. Ge, Y. Chen, *RSC Adv.* **2019**, *9*, 19571.
- [29] A. Fontana, I. Cursaro, G. Carullo, S. Gemma, S. Butini, G. Campiani, *Int. J. Mol. Sci.* **2022**, *23*, 10014.
- [30] M. Brindisi, C. Cavella, S. Brogi, A. Nebbioso, J. Senger, S. Maramai, A. Ciotta, C. Iside, S. Butini, S. Lamponi, E. Novellino, L. Altucci, M. Jung, G. Campiani, S. Gemma, *Future Med. Chem.* **2016**, *8*, 1573.
- [31] G. Campiani, S. Butini, C. Fattorusso, B. Catalanotti, S. Gemma, V. Nacci, E. Morelli, A. Cagnotto, I. Mereghetti, T. Mennini, M. Carli, P. Minetti, M. A. Di Cesare, D. Mastroianni, N. Scafetta, B. Galletti, M. A. Stasi, M. Castorina, L. Pacifici, M. Vertechy, S. D. Serio, O. Ghirardi, O. Tinti, P. Carminati, *J. Med. Chem.* **2004**, *47*, 143.
- [32] G. Campiani, S. Butini, C. Fattorusso, F. Trotta, S. Gemma, B. Catalanotti, V. Nacci, I. Fiorini, A. Cagnotto, I. Mereghetti, T. Mennini, P. Minetti, M. A. Di Cesare, M. A. Stasi, S. Di Serio, O. Ghirardi, O. Tinti, P. Carminati, *J. Med. Chem.* **2005**, *48*, 1705.
- [33] S. Butini, S. Gemma, G. Campiani, S. Franceschini, F. Trotta, M. Borriello, N. Ceres, S. Ros, S. S. Coccone, M. Bernetti, M. De Angelis, M. Brindisi, V. Nacci, I. Fiorini, E. Novellino, A. Cagnotto, T. Mennini, K. Sandager-Nielsen, J. T. Andreasen, J. Scheel-Kruger, J. D. Mikkelsen, C. Fattorusso, *J. Med. Chem.* **2009**, *52*, 151.
- [34] S. Butini, G. Campiani, S. Franceschini, F. Trotta, V. Kumar, E. Guarino, G. Borrelli, I. Fiorini, E. Novellino, C. Fattorusso, M. Persico, N. Orteca, K. Sandager-Nielsen, T. A. Jacobsen, K. Madsen, J. Scheel-Kruger, S. Gemma, *J. Med. Chem.* **2010**, *53*, 4803.
- [35] S. Brogi, A. Ramunno, L. Savi, G. Chemi, G. Alfano, A. Pecorelli, E. Pambianchi, P. Galatello, G. Compagnoni, F. Focher, G. Biamonti, G. Valacchi, S. Butini, S. Gemma, G. Campiani, M. Brindisi, *Eur. J. Med. Chem.* **2017**, *138*, 438.
- [36] M. Brindisi, S. Butini, S. Franceschini, S. Brogi, F. Trotta, S. Ros, A. Cagnotto, M. Salmona, A. Casagni, M. Andreassi, S. Saponara, B. Gorelli, P. Weikop, J. D. Mikkelsen, J. Scheel-Kruger, K. Sandager-Nielsen, E. Novellino, G. Campiani, S. Gemma, *J. Med. Chem.* **2014**, *57*, 9578.
- [37] M. Brindisi, S. Brogi, S. Maramai, A. Grillo, G. Borrelli, S. Butini, E. Novellino, M. Allarà, A. Ligresti, G. Campiani, V. Di Marzo, S. Gemma, *RSC Adv.* **2016**, *6*, 64651.
- [38] S. Federico, T. Khan, A. Fontana, S. Brogi, R. Benedetti, F. Sarno, G. Carullo, A. Pezzotta, A. P. Saraswati, E. Passaro, L. Pozzetti, A. Papa, N. Relitti, S. Gemma, S. Butini, A. Pistocchi, A. Ramunno, F. Vincenzi, K. Varani, V. Tatangelo, L. Patrussi, C. T. Baldari, S. Saponara, B. Gorelli, S. Lamponi, M. Valoti, F. Saccoccia, M. Giannaccari, G. Ruberti, D. Herp, M. Jung, L. Altucci, G. Campiani, *Eur. J. Med. Chem.* **2022**, *238*, 114409.
- [39] N. Relitti, A. P. Saraswati, G. Chemi, M. Brindisi, S. Brogi, D. Herp, K. Schmidtkunz, F. Saccoccia, G. Ruberti, C. Ulivieri, F. Vanni, F. Sarno, L. Altucci, S. Lamponi, M. Jung, S. Gemma, S. Butini, G. Campiani, *Eur. J. Med. Chem.* **2021**, *212*, 112998.
- [40] Y. Xue, B. Gan, Y. Zhou, T. Wang, T. Zhu, X. Peng, X. Zhang, Y. Zhou, *Cell Biochem. Biophys.* **2023**, *81*, 127.
- [41] A. D. Bondarev, M. M. Attwood, J. Jonsson, V. N. Chubarev, V. V. Tarasov, H. B. Schiöth, *Br. J. Clin. Pharmacol.* **2021**, *87*, 4577.
- [42] G. F. Smith, *Prog. Med. Chem.* **2011**, *50*, 1.
- [43] A. Grillo, F. Fezza, G. Chemi, R. Colangeli, S. Brogi, D. Fazio, S. Federico, A. Papa, N. Relitti, R. Di Maio, G. Giorgi, S. Lamponi, M. Valoti, B. Gorelli, S. Saponara, M. Benedusi, A. Pecorelli, P. Minetti, G. Valacchi, S. Butini, G. Campiani, S. Gemma, M. Maccarrone, G. Di Giovanni, *ACS Chem. Neurosci.* **2021**, *12*, 1716.
- [44] J. F. Sánchez-Tejeda, J. F. Sánchez-Ruiz, J. R. Salazar, M. A. Loza-Mejía, *Front. Chem.* **2020**, *8*, 176.
- [45] R. Morphy, C. Kay, Z. Rankovic, *Drug Discov. Today* **2004**, *9*, 641.
- [46] M. Mileni, J. Garfinkle, C. Ezzili, F. S. Kimball, B. F. Cravatt, R. C. Stevens, D. L. Boger, *J. Med. Chem.* **2010**, *53*, 230.
- [47] Y. Hai, D. W. Christianson, *Nat. Chem. Biol.* **2016**, *12*, 741.
- [48] C. Hardouin, M. J. Kelso, F. A. Romero, T. J. Rayl, D. Leung, I. Hwang, B. F. Cravatt, D. L. Boger, *J. Med. Chem.* **2007**, *50*, 3359.
- [49] B. Uttara, A. Singh, P. Zamboni, R. Mahajan, *Curr. Neuropharmacol.* **2009**, *7*, 65.
- [50] D. R. Brown, *Mol. Cell. Neurosci.* **1999**, *13*, 379.
- [51] S. Satarker, S. L. Bojja, P. C. Gurram, J. Mudgal, D. Arora, M. Nampoothiri, *Cells* **2022**, *11*, 1139.
- [52] M. Lei, X. Chen, Y. Wang, L. Zhang, H. Zhu, Z. Wang, *Org. Lett.* **2022**, *24*, 2868.
- [53] R. A. Friesner, R. B. Murphy, M. P. Repasky, L. L. Frye, J. R. Greenwood, T. A. Halgren, P. C. Sanschagrín, D. T. Mainz, *J. Med. Chem.* **2006**, *49*, 6177.
- [54] T. A. Halgren, R. B. Murphy, R. A. Friesner, H. S. Beard, L. L. Frye, W. T. Pollard, J. L. Banks, *J. Med. Chem.* **2004**, *47*, 1750.
- [55] G. Madhavi Sastry, M. Adzhigirey, T. Day, R. Annabhimoju, W. Sherman, *J. Comput.-Aided Mol. Des.* **2013**, *27*, 221.
- [56] M. K. McKinney, B. F. Cravatt, *J. Biol. Chem.* **2003**, *278*, 37393.
- [57] A. Lodola, M. Mor, S. Rivara, C. Christov, G. Tarzia, D. Piomelli, A. J. Mulholland, *Chem. Commun.* **2008**, *14*, 214.
- [58] M. P. Jacobson, R. A. Friesner, Z. Xiang, B. Honig, *J. Mol. Biol.* **2002**, *320*, 597.
- [59] J. Li, R. Abel, K. Zhu, Y. Cao, S. Zhao, R. A. Friesner, *Proteins* **2011**, *79*, 2794.

SUPPORTING INFORMATION

Additional supporting information can be found online in the Supporting Information section at the end of this article.

How to cite this article: A. Papa, I. Cursaro, L. Pozzetti, C. Contri, M. Cappello, S. Pasquini, G. Carullo, A. Ramunno, S. Gemma, K. Varani, S. Butini, G. Campiani, F. Vincenzi, *Arch. Pharm.* **2023**, e2300410.

<https://doi.org/10.1002/ardp.202300410>